VILNIUS UNIVERSITY

LIFE SCIENCES CENTRE

NATALIIA NELSON

Knock-In of Genetically Encoded EM Reporters in Human Cells through CRISPR-Cas9 Nuclease.

Master's Thesis

Genetics Study Program

Supervisor

Dr. Jonathan Lee Arias Fuenzalida

Vilnius 2024

TABLE OF CONTENTS

ABBREVIATIONS

EM – Electron Microscopy.

POI – protein or molecule of interest.

APX – ascorbate peroxidase.

APEX – enhanced APX.

ER – endoplasmic reticulum.

AuNP – golden nanoparticles.

MT – Metallothionein.

SNR – signal-to-noise ratio.

ANSM – auto-nucleation suppression mechanism.

BSM – Brust-Schiffrin method.

RSH – thiol ligands.

MTn – aldehyde-fixative-resistant variant of MT.

COX8A – cytochrome c oxidase subunit 8A.

IMM – inner mitochondrial membrane.

RC – respiratory chain.

ATP – adenosine triphosphate.

ADP – adenosine diphosphate.

OxPhos – oxidative phosphorylation.

KDEL – Lys-Asp-Glu-Leu sequence.

KDELR – KDEL receptor.

CD – cluster of differentiation.

TCR – T-cell receptor.

MHCI – major histocompatibility complex I.

NKG2D – natural killer gene 2D.

GA – Gibson Assembly.

AmpR – ampicillin resistance gene.

AAV – adeno-associated virus.

PURO – puromycin resistance gene.

CMV – cytomegalovirus.

PolyA – polyadenylation sequence.

CRISPR – a clustered regularly interspaced short palindromic repeat.

Cas – CRISPR associated.

tracrRNA – trans-activation CRISPR RNA.

crRNA – CRISPR RNA.

sgRNA – single-guide RNA.

PAM – protospacer-adjacent motif.

NHEJ – non-homologous end joining pathway.

HDR – homology-directed repair pathway.

DSB – double-strand DNA break.

KI – knock-in.

FCM – flow cytometry.

VILNIUS UNIVERSITY

LIFE SCIENCES CENTRE

Nataliia Nelson

Knock-In of Genetically Encoded EM Reporters in Human Cells through CRISPR-Cas9 Nuclease.

Master's thesis

SUMMARY

Single-protein tracking can provide crucial information about cell biology. Electron microscopy can visualize molecules with higher resolution, than widely used fluorescent microscopy. To visualize specific proteins, EM tags are needed to introduce into the cells. CRISPR-Cas9 technology, derived from *S.pyogenes*, revolutionized the gene engineering approaches. It allowed for the precise and easy knock-in of the donor DNA sequences.

EM tags for single proteins should localize molecules with high precision and give a low signal-to-noise ratio on the EM images. One of the most suitable tags for single-protein visualization is metallothionein. The application of this tag was checked in procaryotic and eukaryotic mammal cells. For a better understanding of disease and drug development, it is important to localize molecules in human cells.

We successfully cloned EM reporters for visualization of mitochondria, endoplasmic reticulum, and inner and outer membranes of the human cells, and quality controlled them with Sangar sequencing.

VILNIAUS UNIVERSITETAS

GYVENIMO MOKSLŲ CENTRAS

Natalija Nelson

Genetiškai užkoduotų EM reporterių įtraukimas į žmogaus ląsteles per CRISPR-Cas9 nukleazę.

Magistro baigiamasis darbas

SANTRAUKA

Vieno baltymo sekimas gali suteikti esminės informacijos apie ląstelių biologiją. Elektroninė mikroskopija gali vizualizuoti molekules didesne skiriamąja geba nei plačiai naudojama fluorescencinė mikroskopija. Norint vizualizuoti specifinius baltymus, į ląsteles reikia įvesti EM žymes. CRISPR-Cas9 technologija, gauta iš S.pyogenes, pakeitė genų inžinerijos metodus. Tai leido tiksliai ir lengvai nustatyti donoro DNR sekas.

Pavienių baltymų EM žymos turėtų labai tiksliai lokalizuoti molekules ir EM vaizduose suteikti mažą signalo ir triukšmo santykį. Viena iš tinkamiausių žymenų vieno baltymo vizualizacijai yra metalotioneinas. Šios žymos pritaikymas buvo patikrintas prokariotinėse ir eukariotinėse žinduolių ląstelėse. Norint geriau suprasti ligas ir vaistų vystymąsi, svarbu lokalizuoti molekules žmogaus ląstelėse.

Sėkmingai klonavome EM reporterius, kad galėtume vizualizuoti žmogaus ląstelių mitochondrijas, endoplazminį tinklą ir vidines bei išorines membranas, o jų kokybę kontroliavome naudodami Sangar sekos nustatymą.

INTRODUCTION

CRISPR-Cas9 nucleases changed gene engineering techniques, allowing for the modification of the genome with high efficiency and precision. CRISPR-Cas9 could be used for editing the genome in various organisms, for studying diseases and gene therapy, for detecting gene activity during a disease (Barman et al., 2020). It has been studied as a possible tool for gene therapy in a wide range of diseases, such as cancer, heart-related diseases, infections, and immune system illnesses (Karimian et al., 2019; Strong & Musunuru, 2017; Xiong et al., 2016).

As a result of CRISPR-Cas9 activity, double-strand DNA break (DSB) occurs, which commences a non-homologous end joining (NHEJ) or a homology-directed repair (HDR) mechanism (Ran, Hsu, Lin, et al., 2013; Smirnikhina et al., 2019). During NHEJ, that happens during the G1 and late G2 phases of the cell cycle, the DSB is recognized, and special complexes attract polymerases, nucleases, and ligases to restore DNA sequence. As a result, insertions or deletions of several nucleotides can occur (Davis & Chen, 2013; Watanabe & Lieber, 2023). During HDR, DSB is restored with the help of homologous DNA sequence, a second chromosome or donor DNA. HDR takes place after DNA replication, in the S/G2 phase of the cell cycle, and allows insertion of a DNA sequence into the genome (Barman et al., 2020; Smirnikhina et al., 2019).

To induce knock-in (KI) of the DNA donor sequences into the genome, an increase of HDR rate is needed. Inhibition of NHEJ, reduction of the expression of its proteins, and stimulation of HDR subunits could achieve a rise of KI efficiency (Banan, 2020; Smirnikhina et al., 2019).

Single protein tracking and visualization can enlighten cellular mechanisms of protein secretion, cell-cell interaction, and disease and infection mechanisms. Fluorescent microscopy had a great impact on the understanding of cell biology on the molecular level (S.-L. Liu et al., 2020). In eukaryotic cells, protein function is tightly connected to its localization within the cell, as each compartment provides different microenvironment conditions, such as different pH and redox conditions (Lundberg & Borner, 2019).

Electron microscopy (EM) can provide a protein visualization image with high resolution (Koster & Klumperman, 2003). For EM protein imaging signal-dense tags are needed (Kikkawa & Yanagisawa, 2022). There are several different approaches to visualize proteins with prokaryotic and eukaryotic cells (Martell et al., 2012; Vázquez-Gutiérrez & Langton, 2015), however, the most promising EM tag for single-protein tracking is metallothionein (Jiang et al., 2020). Jiang et al visualized proteins in prokaryotic cells, mitochondria, and endoplasmic reticulum organelles within mammalian cells.

For a better understanding of protein interactions and disease and drug development within human cells, it is necessary to localize proteins with high precision. KI of EM reporters in human cells can give valuable insight into protein-protein interactions and cellular pathways.

Aim of the thesis:

To create EM reporters for localization of mitochondria, endoplasmic reticulum, and inner and outer cell membrane organelles in the human cells.

Objectives:

- To create gBlocks of EM reporters.
- To prepare a maxiprep of EM reporters.
- To create a cell culture system compatible with reporter knock-in.
- To electroporate EM reporters onto the cell culture.
- Analyzing electroporated cells with flow cytometry.

1. LITERATURE REVIEW

1.1. Electron microscopy

Electron microscopy (EM) is the most commonly used technique to obtain images of the cellular structure, and combined with protein-detection methods it is the only technique to provide a visualization of proteins of interest (POIs) and their interactions with high resolution (Koster & Klumperman, 2003). Rapid-freezing and freeze substitution allow to visualize cellular structure with unprecedented detail and reliability, providing EM images in close resemblance with the living state of the cells. (McIntosh, 2001)

In order to highlight POIs, EM tagging is needed. To be an adequate tag for EM, molecules should meet 5 requirements: low perturbation, low false-positive rate, low false-negative rate, spatial accuracy, and high signal-to-noise ratio. Low perturbation means that the molecule should be small enough not to disrupt the cell structure. False-positive rate describes the ability of the tag to bind with other proteins in the cell other than POIs. False-negative rate describes the number of POIs that are bound to the tag. To visualize the precise position of POI the distance between the electron visible part of the tag and the molecule of interest should not be long. Because the cell structure is visible in electron microscopy, tags for visualizing molecules should have higher electron density (Kikkawa & Yanagisawa, 2022).

1.2. Tags

1.2.1. APEX

An engineered variant of ascorbate peroxidase (APX), enhanced APX (APEX), is a monomeric heme enzyme, that tolerates strong fixation procedures for EM. It is used for EM visualization of cellular compartments in the cells. APEX showed a strong contrast in staining mitochondria and endoplasmic reticulum (ER) lumen (Martell et al., 2012). In this paper, Martell et al. described a possible limitation of APEX application. APEX requires a heme cofactor for its activation, therefore in heme-poor conditions, APEX can show insufficient activity for EM. APEX2, a variant of APEX, produces stronger EM contrast, than APEX, and can be used for EM visualization of a wide range of proteins and cellular compartments, such as proteins of cytoskeleton, Golgi apparatus, endosomes, etc. (Martell et al., 2017; Sengupta et al., 2019)

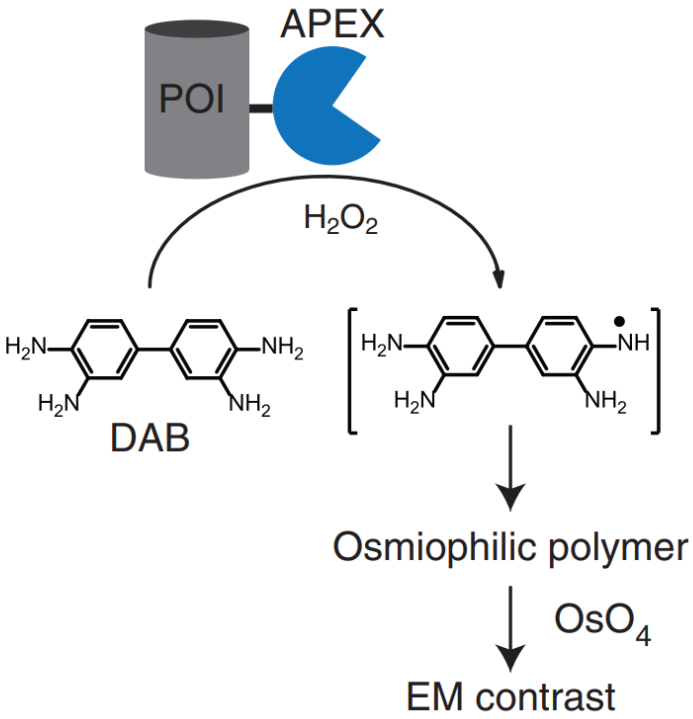

Figure 1.1. Schematic representation of the formation of EM contrast by APEX using DAB and OsO_4 treatment. The picture was published by Martell et al., 2012. https://doi.org/10.1038/nbt.2375

As it is shown in Figure 1.1 in live cells, the APEX reporter triggers the oxidative polymerization of diaminobenzidine (DAB) upon exposure to H_2O_2, resulting in the localized precipitate. Subsequent staining with osmium tetroxide (OsO_4) improves EM contrast, improving the visualization of POI and its subcellular interactions (Martell et al., 2012)

1.2.2. Immunogold EM

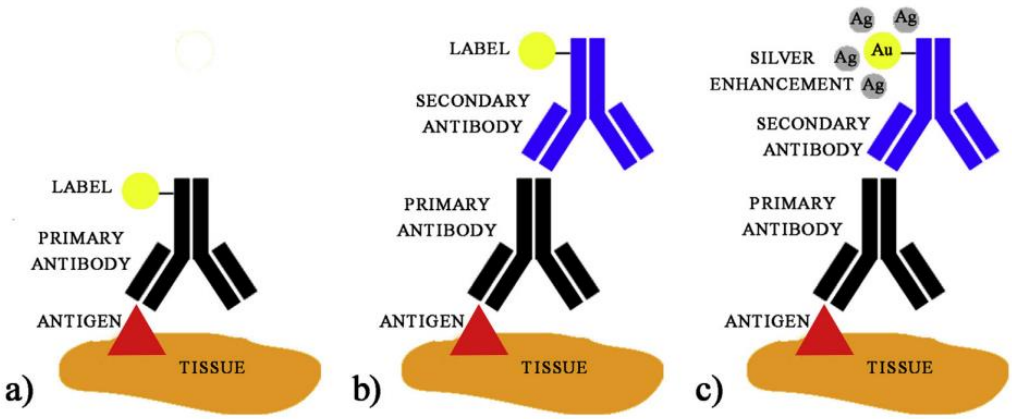

Figure 1.2. Schematic representation of the immunolabeling mechanisms. a) Direct labeling. b) Indirect labeling; c) Silver-enhanced indirect immunogold labeling. The picture was published in Vázquez-Gutiérrez & Langton, 2015. http://dx.doi.org/10.1016/j.tifs.2014.10.002

In immunogold EM specific antibodies are used for the labeling of POIs. There are different labeling techniques for immunogold EM, direct and indirect labeling. As shown in figure 1.2 direct labeling means golden nanoparticles (AuNPs), which provide a visible EM signal, are being attached to the primary antibody, whereas indirect labeling means that there is a secondary antibody with AuNP attached to the primary antibody. Furthermore, silver-enhancing could take place to make a stronger EM signal (Gulati et al., 2019; Sachse et al., 2024; Vázquez-Gutiérrez & Langton, 2015). The disadvantages of the immunogold technique are the specificity of antibodies, the availability of them, and tissue preparation. If the antibody is not specific to the POI, it will attach to other molecules producing non-specific signals, so the false-positive rate could be high. Moreover, immunogold labels are relatively big and therefore cannot provide a precise localization of POIs. (Shigemoto, 2022)

Most of the known EM tags are used to visualize subcellular compartments, however, there are several EM tags that can show single molecules in the cell, for example, Ferritag and Metallothionein (MT). The main drawback of such tags is background signal noise. Moreover, MT is the only adequate tag for single-protein localization, due to Ferritag is considered to be too large (Shigemoto, 2022)

1.3. Metallothionein

MTs are an intracellular cysteine-rich family of proteins. They bind to heavy metals in the cell, prevent their toxicity in organisms, have antioxidant properties, and play an important role in scavenging free radicals. MTs have been used in biomedical and biotechnological fields as biomarkers, biosensors, and as a treatment for heavy metal contamination (Samuel et al., 2021; Thirumoorthy et al., 2007). MTs have 2 binding domains α and β with several binding sites in them as shown in figure 1.3 (Krężel & Maret, 2021).

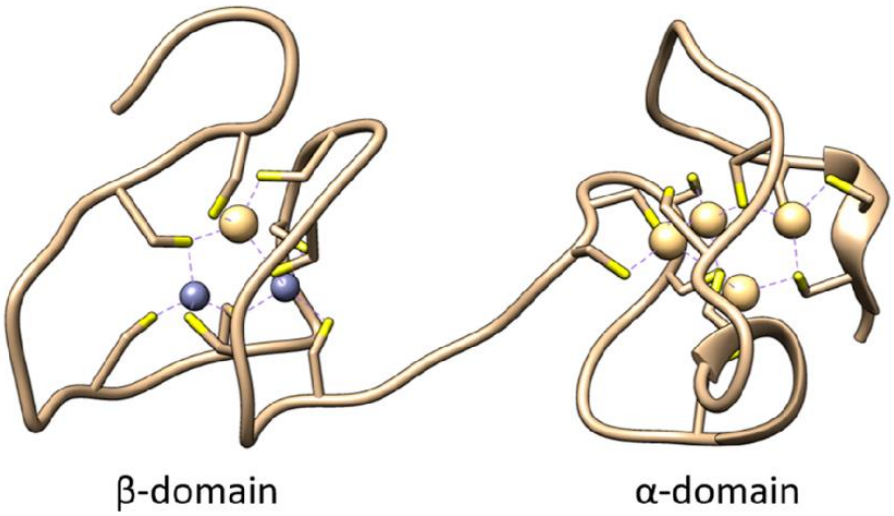

Figure 1.3. Schematic representation of the metallothionein structure. The picture was published in Krężel & Maret, 2021. https://doi.org/10.1021/acs.chemrev.1c00371

MTs are relatively small (from 0.5 to 14 kDa) family of proteins, that can be used as a benign, cloneable tag for visualization of POIs in EM. MT as an EM tag provides a good signal-to-noise ratio (SNR), a small size and low molecular weight, and a tightly focused signal (Morphew et al., 2015).

In 2009 Diestra et al. found that MT tags generate small electron-dense particles in vivo after being treated with gold nanoparticles. The smallest was estimated to be about 1 nm, which tells that the localization of POIs with MT tags can be very precise. The ability of MT to bind to heavy metals, including gold, allows for the formation of electron-dense particles and therefore allows to use of MT as a cloneable tag for EM. Moreover, MT can be used for studying single protein arrangement in 3D reconstruction using EM tomography and macromolecular interactions that support cellular functions. Furthermore, MT tags are applicable both for viruses and eukaryotic cells (Diestra et al., 2009). The composite of the modification of MT and AuNP has transmembrane ability, antioxidant activity, and stability (Li et al., 2024)

The drawback of MT as an EM tag is that in the cell it is possible to have background signals. It can be eliminated by using an auto-nucleation suppression mechanism (ANSM). (Shigemoto, 2022)

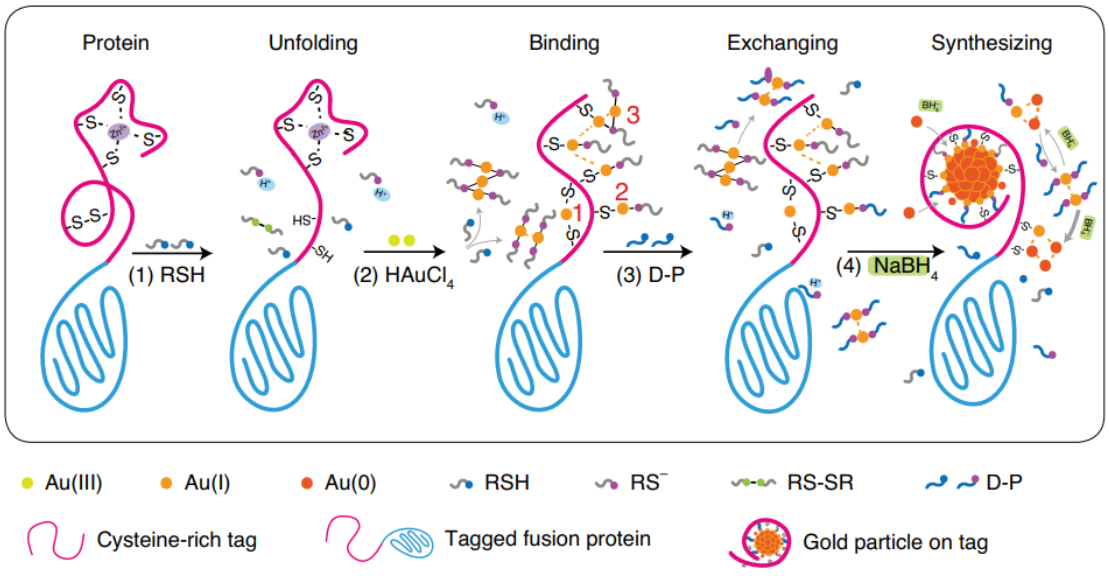

Figure 1.4. Schematic representation of the formation of EM-dense signal on the MT tag with AuNP according to the Brust-Schiffrin method. The picture was published by Jiang et al., 2020. https://doi.org/10.1038/s41592-020-0911-z

The Brust-Schiffrin method (BSM) is mainly used for the synthesis of thiolate-capped AuNP. At its core, BSM has two reduction steps: first, thiol ligands (RSH) reduce HAuCl4 to create thiolate-Au(I) polymers, and then NaBH4 reduces them to form AuNP (Brust et al., 1994). In figure 1.4 there is a schematic representation of AuNP synthesis, based on BSM.

In 2020 Jiang et al. developed an aldehyde-fixative-resistant variant of MT (MTn) and designed a new method to synthesize AuNP based on the BSM. They discovered an ANSM that ensures that EM-visible AuNPs are synthesized on cysteine-rich tags. To prevent the creation of off-target AuNP Jiang et al suggested using BSM in the condition of thiolate anions-to-Au ratio ≥ 2/1, which can be modified by changing an initial concentration of RSH and pH. They successfully applied both MTn tag and ANSM in prokaryotic *E.coli*, in outer membranes of the ER, nuclear pores, and spindle pore body in eukaryotic yeast *S.pombe*, and in ER lumen, ER membrane, mitochondrial matrix in mammalian cells. They stated that their AuNP synthesis protocol achieved higher labeling efficiency than classical immune-EM. However, they expressed the main limitation of their methods as well. Firstly, the cysteine-rich tags that are expressed in the reducing compartments are unfolded, which make them sensible to aldehyde fixatives. Secondly, permeabilization is used for the penetration of gold precursors through the cell membrane, which can cause ultrastructural distortion.

1.4 Proteins of interest

1.4.1. COX8A

COX8A is a cytochrome c oxidase subunit 8A. It is an integral protein that is localized in the inner membrane of the mitochondria (IMM) and is a subunit of complex IV in the respiratory chain (RC). COX8A is to localize and visualize mitochondria and its cristae (Stephan et al., 2019).

14 COX subunits play a role in the RC in mammalian cells, and the core complex consists of mitochondrial-encoded proteins COX1, COX2, and COX3. The rest 11 proteins are nuclear encoded, including COX8A. These subunits regulate the COX formation, stabilization, and functional interaction with other proteins (Ramzan et al., 2021; Rotko et al., 2021). In their study, Rotko et al found that a deficiency of COX8A protein in the cells results in the destabilization of COX monomers and dimers.

RC is located in the flat regions of IMM, and its main function is the transfer of electrons from low-potential electron donors to high-potential electron acceptors. As a result, the voltage difference is maintained between the mitochondrial matrix and inner mitochondrial space, providing energy to transform adenosine triphosphate (ATP) from adenosine diphosphate (ADP) by ATP-

synthase (Brzezinski et al., 2021). RC alongside ATP-synthase is a part of the oxidative phosphorylation system (OxPhos). A schematic representation of OxPhos can be seen in figure 1.5.

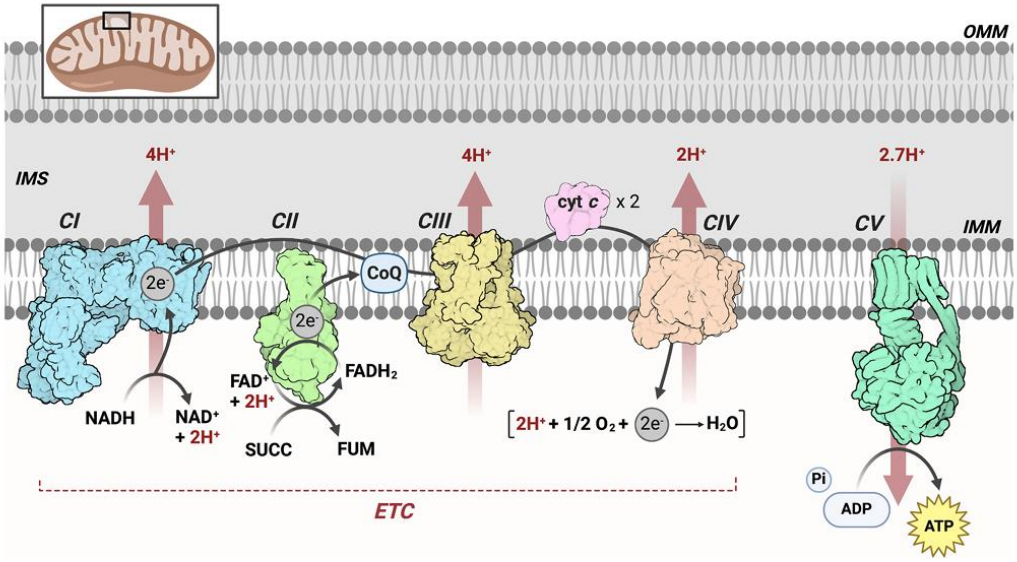

Figure 1.5. Schematic representation of oxidative phosphorylation (OxPhos) system. IMM – inner mitochondrial membrane; OMM – outer mitochondrial membrane; IMS – inter mitochondrial space; ETC – electron transport chain, otherwise known as a respiratory chain; CI-CV – complexes I-V of OxPhos system. The picture was published in Brischigliaro & Zeviani, 2021. https://doi.org/10.1016/j.bbabio.2020.148335

1.4.2. KDEL

KDEL is a sequence of amino acids Lys-Asp-Glu-Leu. It localizes on the C-terminus of the protein. When a protein with such a sequence escapes the ER to the Golgi apparatus, the KDEL receptor (KDELR) recognizes this sequence and ensures its transfer back to the ER. As shown in figure 1.6 KDELR transfers the protein back with the protection of COPI-coated vesicles. An empty KDELR receptor then moves back to the Golgi apparatus with the help of COPII-coated vesicles. (Gerondopoulos et al., 2021; Newstead & Barr, 2020).

KDELR recognizes and binds to KDEL-containing proteins through the pH-dependent mechanism. In the acidic environment of the Golgi apparatus, KDELR becomes protonated, which allows it to create a hydrogen bond between the KDEL sequence and its receptor. At neutral pH of ER KDELR undergoes deprotonation, which destabilizes the hydrogen bond (Newstead & Barr, 2020).

KDELR retrieval pathway maintains ER resident proteins within the ER lumen. When the cell encounters stress, it triggers adaptive responses that activate the protective functions of the KDELR pathway (Tapia et al., 2019; Wires et al., 2021).

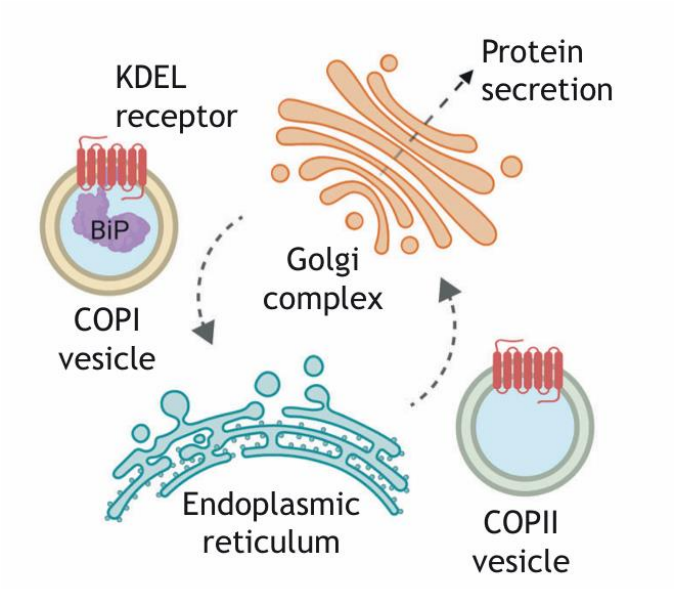

Figure 1.6. Schematic representation of KDEL receptor function. The picture was published in (Newstead & Barr, 2020). https://doi.org/10.1242/jcs.250100

1.4.3. CD proteins

CD molecules, known as clusters of differentiation, are expressed on the cellular membrane of the immune system cells and play a role in the cell-cell interaction (Kalina et al., 2019).

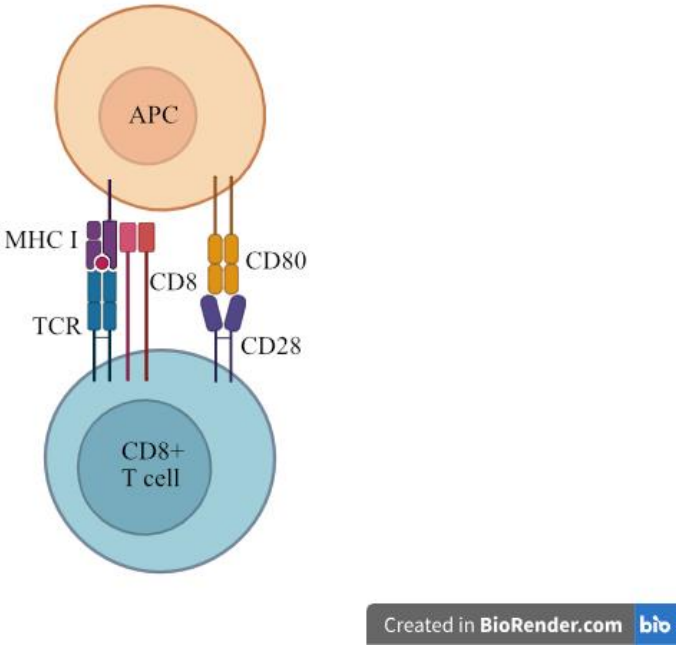

Figure 1.7. Schematic representation of CD8+ T-cell bound with a cancer cell. T-cell receptor (TCR) bound with major histocompatibility complex I (MHCI), CD8 protein acts as a co-receptor.

CD28 is bound to CD80 on the antigen-presenting cell (APC). The picture was created with BioRender.com.

CD8 proteins are transmembrane glycoproteins, that act as co-receptors alongside with T-cell receptor (TCR) as shown in figure 1.7. CD8 proteins could be found on the cellular membrane of the cytotoxic T-cells, and they could bind to major histocompatibility complex I (MHCI) present in the antigen-presenting cells (Koh et al., 2023; Reina-Campos et al., 2021). CD8+T-cells express CD28, which binds to the CD80 and CD86 of the antigen-presenting cells. CD28 produces an activating signal for T-cells (Esensten et al., 2016).

Natural killer gene 2D (NKG2D), also known as CD314 (Hassona et al., 2021; Kim et al., 2020), is an activating receptor, that binds to the diverse range of ligand molecules, that are being upregulated during cell stress response. NKG2D is present in NK cells, NK T-cells, and memory CD8+ TCRαβ T-cells and acts as a "master switch" in regulating the activation of NK cells (H. Liu et al., 2019).

1.5. The theory behind the methods and their analysis.

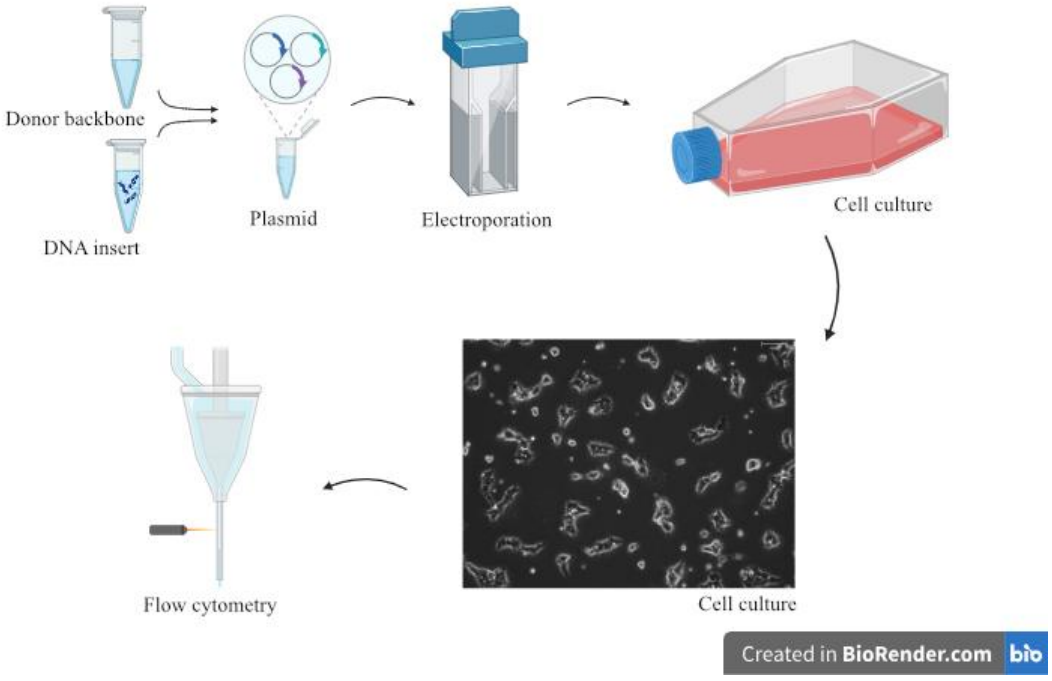

Figure 1.8. Schematic representation of the EM reporters knock-in in the human cells. The picture was created with BioRender.com.

In figure 1.8 the main workflow of the knock-in strategy is presented. First, EM reporters with MTn as an EM tag and a green fluorescent protein (GFP) in their sequence were created. Then, they were introduced into the donor plasmid backbone, which could allow the reporters to enter human

cells. Combined plasmids could be used for electroporation into the compatible cell culture. After cell culture recovery and expansion, EM reporters could be checked with flow cytometry.

1.5.1. TOPO blunt cloning

TOPO cloning is a one-step technique, that allows the insertion of DNA fragments into a linearized vector using topoisomerase I enzyme, which is activated in this reaction by CCCTT overhang. At room temperature, topoisomerase I act as a restriction enzyme and has an ability to ligase the DNA. The principle of TOPO-Blunt cloning is shown in figure 1.9. Blunt TOPO cloning is a non-directional method because, on both ends of the vector, there is CCCTT overhang. The accuracy of this method is 90% (Choi et al., 2019, p. 113; Li et al., 2022; Patel, 2009). TOPO-Blunt-II backbone has a kanamycin antibiotic resistance.

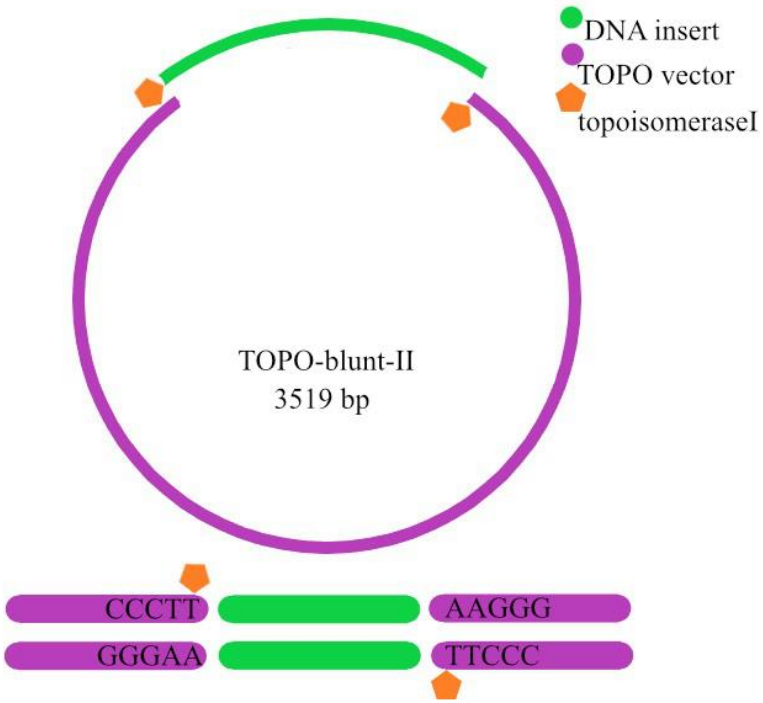

Figure 1.9. Schematic representation of TOPO-blunt-II cloning technique. The topoisomerase I enzyme acts both as a restriction enzyme and DNA ligase.

1.5.2. Gibson assembly

Gibson assembly (GA) is a cloning technique that allows the binding of several inserts in a particular order in one reaction using 5'-exonuclease, a DNA polymerase, and a DNA ligase (Gibson et al., 2009). The accuracy of the GA cloning is 90-95% and decreases with cloning three or more fragments (Li et al., 2022, p. 202).

The main principle of the GA as is shown in figure 1.10 requires a 5'-exonuclease that chews back nucleotides from the 5' end. Generated 3' ends are complementary to each other and can be

annealed, and a double-stranded DNA then are repaired with DNA polymerase and ligase at 50°C (Gibson et al., 2009).

GA is widely used to clone DNA sequences, for DNA library and new clone construction (Bordat et al., 2015; Thomas et al., 2015).

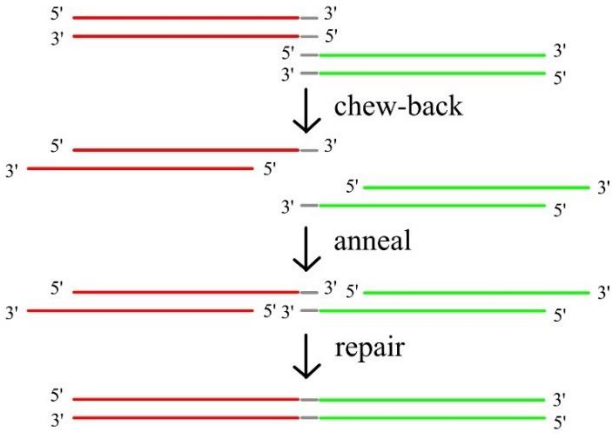

Figure 1.10. Schematic representation of the Gibson Assembly reaction.

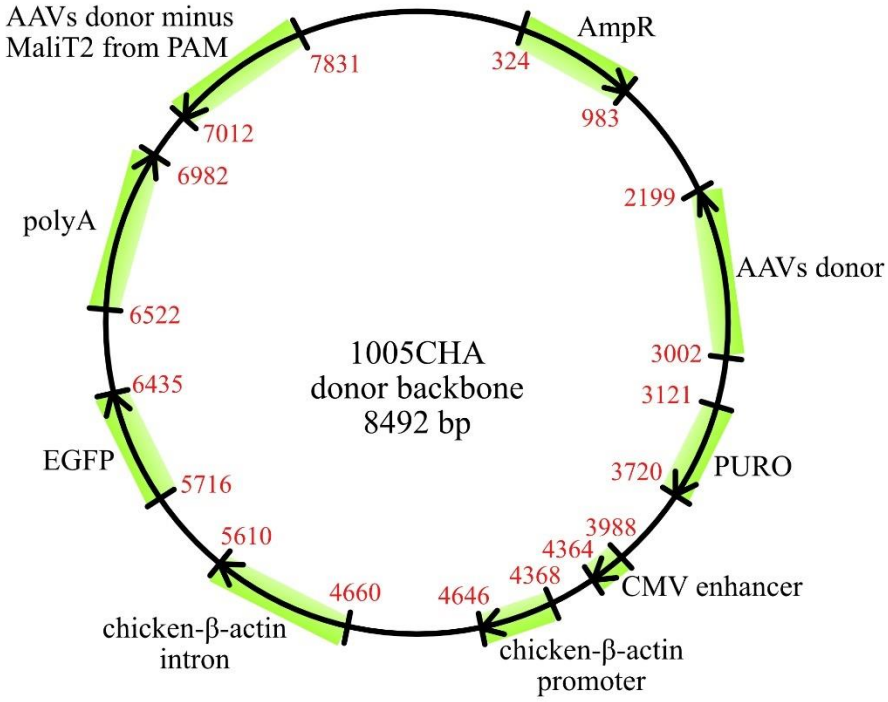

Figure 1.11. Schematic representation of 1005CHA donor backbone. AmpR – ampicillin resistance gene; AAVs – adeno-associated virus; PURO – puromycin resistance gene; CMV –

cytomegalovirus gene; EGFP – green fluorescent protein; polyA – polyadenylation; PAM – short protospacer-adjacent motif. The donor was taken from Mali et al., 2013.

In figure 1.11 there is a schematic representation of the donor backbone (Mali et al., 2013), that was used for GA. There are several features in the donor sequence, such as ampicillin and its analog carbenicillin resistance gene (AmpR) (F. Xu et al., 2024); adeno-associated virus (AAVs), frequently used in gene editing and gene therapy as a vector delivery (Wang et al., 2019); puromycin (PURO) resistance gene (Iwamoto et al., 2014); cytomegalovirus (CMV) enhancer and chicken-β-actin enhance transgene expression (Alexopoulou et al., 2008; Gruh et al., 2008); and polyadenylation sequence (polyA) enhances the efficiency of CRISPR-Cas9 system (Mu et al., 2019).

1.5.3. CRISPR-Cas9

A clustered regularly interspaced short palindromic repeat-associated system (CRISPR-Cas system) is an adaptive immune response system in bacteria and archaea, that protect the cells from intervening with foreign DNA. This system consists of CRISPR repeat-spacer arrays, trans-activation CRISPR RNA (tracrRNA), and CRISPR-associated (Cas) proteins with endonuclease activity (Mali et al., 2013; Y. Xu & Li, 2020). Foreign DNA when entering a prokaryote can be cut by Cas proteins into small fragments and integrated into the CRISPR array as new spacers. Upon invading with the same foreign DNA, CRISPR RNA (crRNA) recognizes it, and the Cas protein cleaves foreign DNA protecting the procaryote (S. Makarova et al., 2011).

CRISPR-Cas9 system, an engineered system derived from *Streptococcus pyogenes*, is rapid, sequence-specific, precise, and the most used of all CRISPR-Cas systems. It consists of an RNA-guided Cas9 protein and a single-guide RNA (sgRNA) (Mali et al., 2013; Ran, Hsu, Wright, et al., 2013). The main principle of CRISPR-Cas9 is shown in figure 1.12. SgRNA detects a short protospacer-adjacent motif (PAM), a 5'-NGG. SgRNA guides Cas9 endonuclease, where Cas9 cleaves the target DNA with two nuclease domains HNH (His-Asn-His) and RuvC. After cleavage, DNA is repaired with one of the two pathways non-homologous end joining (NHEJ) and homology-directed repair (HDR) (Hockemeyer & Jaenisch, 2016; Janik et al., 2020; Ran, Hsu, Wright, et al., 2013).

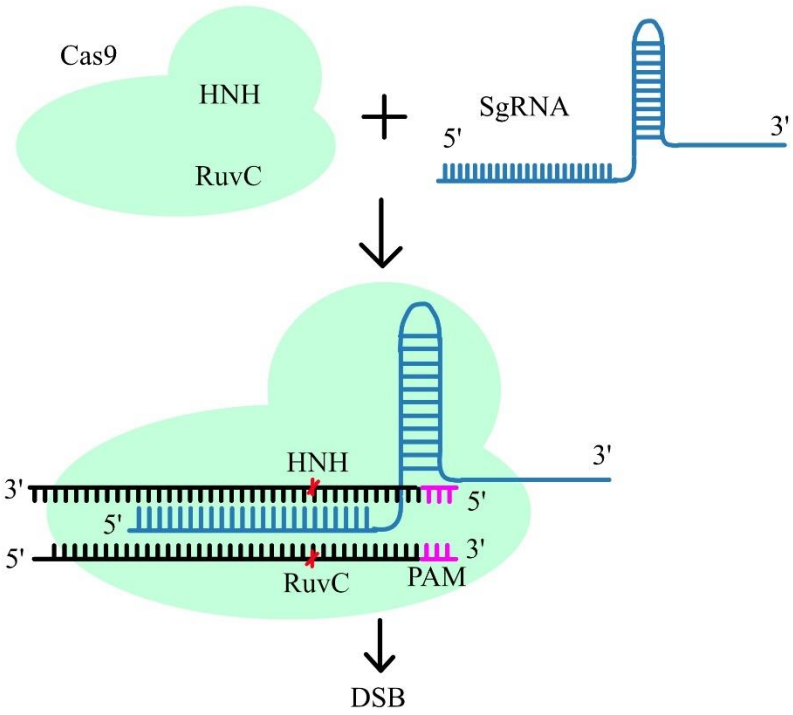

Figure 1.12. Schematic representation of CRISPR-Cas9 gene editing technology. SgRNA – single-guide RNA; HNH – His-Asn-His nuclease domain; RuvC – nuclease domain; PAM – a short protospacer-adjacent motif; DSB – double-stranded breakage of DNA.

CRISPR-Cas9 has a very broad application, varies from creating animal and cell models of human diseases to disease diagnosis and gene therapy (Gould, 2024; Hockemeyer & Jaenisch, 2016; Y. Xu & Li, 2020). Furthermore, CRISPR-Cas9 technology could be used for knock-in and knock-out in the genome by inhibiting or enhancing DNA repair mechanisms (Arias-Fuenzalida et al., 2017; Lau et al., 2020).

1.5.4. Gel electrophoresis

Gel electrophoresis is a gold standard technique to separate, analyze, and purify biological molecules, such as DNA, RNA, and proteins based on their size. DNA molecules have a negative charge, therefore in gel electrophoreses, they move from a negative towards a positive electrode (Syaifudin, 2021). The location of the DNA molecules can be visualized by staining with special intercalating dyes, such as ethidium bromide or SYBR Safe. DNA molecules have a standard mass/charge ratio, therefore the distribution of the molecules by size in agarose gel occurs proportionally to their molecular weight. DNA molecules from 50 bp up to several megabases in length could be separated and visualized on the agarose gel electrophoresis (Green & Sambrook, 2019; Lee et al., 2012; Voytas, 2000).

1.5.5. Flow cytometry

Flow cytometry (FCM) is a technique for single-cell analysis using light scattering, the deflection of the light by a molecule, and fluorescent light signals. It has a broad application: immunology, microbiology, cancer biology, molecular biology, and diagnostics (Bajgelman, 2019; Blair et al., 2019; McKinnon, 2018).

The principle of the FCM includes cell transferring through a capillary with a light source, and photodetectors capture scattered light allowing the analysis of cell size, granularity, and expression of the molecules in them. Fluorescent molecules have a range of different wavelengths of scattered light, which allows several fluorescent compounds to be used at the same time (Adan et al., 2017; Bajgelman, 2019). Cells are treated and transformed with fluorescent proteins, fluorescent dyes, or immunostaining with fluorescent antibodies to prepare the cells for fluorescent analysis. The most commonly used fluorescent protein is a GFP, secreted from the jellyfish (Adan et al., 2017; McKinnon, 2018). FCM results are analyzed graphically with histograms and dot plots using R-based software (Bajgelman, 2019; Montante & Brinkman, 2019).

2. MATERIALS AND METHODS

2.1. Materials

2.1.1. Samples

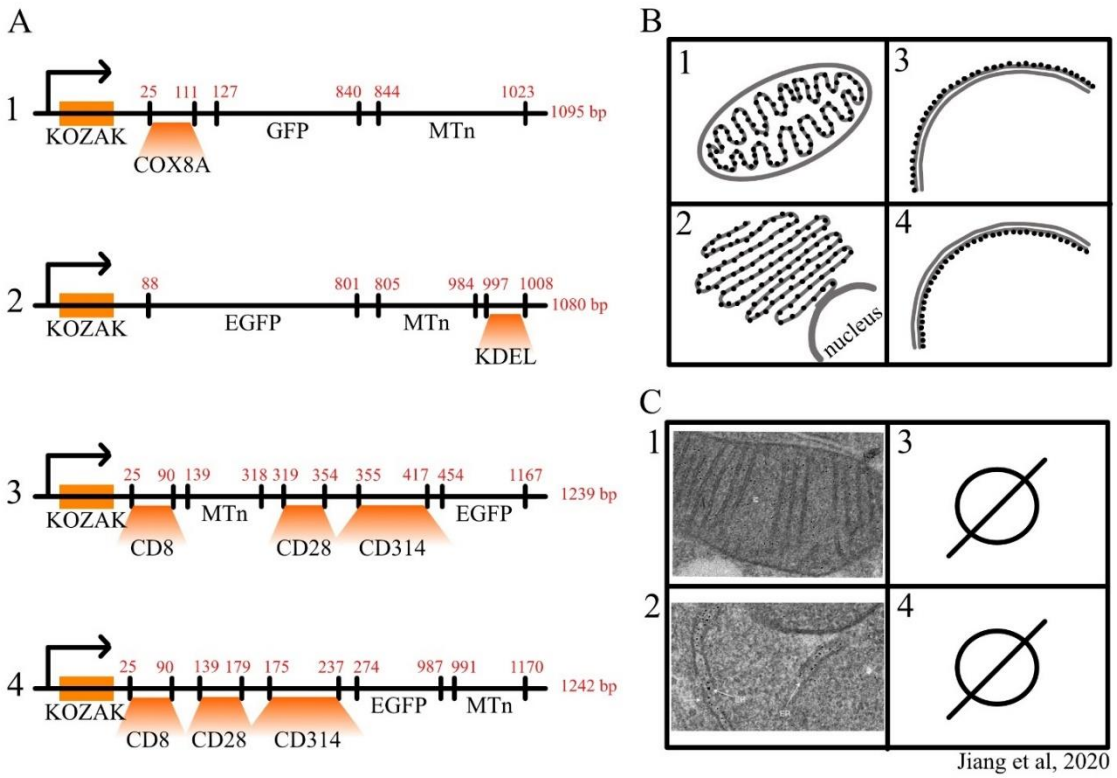

Figure 2.1. Schematic representation of the EM reporters. A – schemes of the gene sequences. 1 – S050-COX8A-MTn; 2 – S051-KDEL-MTn; 3 – S052-MTn-CD8; 4 – S053-CD8-MTn. GFP and EGFP – green fluorescent proteins; MTn – metallothionein. B – schematic pictures of the localization of the POIs. 1 – mitochondria; 2 – endoplasmic reticulum; 3 – outer cell membrane; 4 – inner cell membrane. C – pictures from the Jiang et al paper. 1 – mitochondria; 2 – endoplasmic reticulum.

As it is represented in figure 2.1 four EM reporters were made to localize mitochondria with COX8A protein, endoplasmic reticulum with KDEL, and outer and inner cell membrane with CD proteins. EM sensors for mitochondria and ER localization were made according to the Jiang et al paper of 2020, EM images of mitochondria and ER proteins were taken from Jiang et al. paper, 2020.

2.1.2. Reagents

dNTP Mixture was obtained in Takara and was stored at -20 °C.

PrimeSTAR GXL DNA Polymerase 250 U with catalog number R050A was obtained in Takara, LineaLibera, and was stored at -20 °C.

5X PrimeSTAR (Mg2 + plus) was obtained in Takara and was stored at -20 °C.

4LT TAE (10X), TRIS + acetate + EDTA 4L with catalog number J63677.K7 was obtained in Thermo Scientific, FisherScientific.

Topvision agarose with catalog number R0492 was obtained in Thermo Scientific, FisherScientific.

SYBR Safe DNA Gel Stain, 400 µL, 10000x with catalog number S33102 was obtained in Invitrogen, Linealibera.

GeneRuler 1kb DNA Ladder with catalog number SM0313 was obtained in Thermo Scientific, FisherScientific, and was stored at -4 °C.

6X TriTrack DNA Loading Dye with catalog number R1161 was obtained in Thermo Scientific, FisherScientific, and was stored at -4 °C.

GeneJET Gel Extraction Kit with catalog number K0692 was obtained in Thermo Scientific, LineaLibera.

Salt solution from Zero Blunt TOPO PCR Cloning Kit with catalog number 46-0205 was obtained in Invitrogen, LineaLibera and was stored at -20 °C.

PCR-BluntII-TOPO from Zero Blunt TOPO PCR Cloning Kit with catalog number 100023351 was obtained in Invitrogen, LineaLibera and was stored at -20 °C.

Competent E. coli stellar cells with catalog number 636763 were obtained in Takara and were stored at -80 °C.

LB broth, pH 7.3-7.7, with catalog number P000062428 was obtained in Biolab, Grida and stored at -4 °C.

LB agar with catalog number P000062428 was obtained in Biolab, Grida and stored at -4 °C.

The antibiotic Kanamycin Sulfate with catalog number P000062575 was obtained in Tocris, Grida and stored at -20 °C.

DreamTaq Green PCR Master Mix (2X) with catalog number K1081 was obtained in Thermo Scientific, FisherScientific and stored at -20 °C.

T7 promoter sequencing primer, 20-mer with catalog number SO118 was obtained in Thermo Scientific and stored at -20 °C.

SP6 promoter sequencing primer, 18-mer with catalog number SO116 was obtained in Thermo Scientific and stored at -20 °C.

Glycerol 99%, 500 ml with catalog number G5516-500ML was obtained in Sigma, LaboChema, autoclaved and stored at -4 °C.

QIAprep Spin Miniprep Kit (250) with catalog number 172018067 was obtained in Qiagen, LineaLibera.

Gibson Assembly Master Mix 2X with catalog number M5510AA was obtained in NEB and stored at -20 °C.

The antibiotic carbenicillin disodium salt 1g with catalog number P000062629 was obtained in Grida and stored at -4 °C. The solution of the antibiotic was stored at -20 °C.

HiSpeed Plasmid Maxi Kit (25) with catalog number 12663 was obtained in Qiagen, LineaLibera.

Isopropanol (2-Propanol), 1L with catalog number 190764-1L was obtained in Honeywell, Labochema.

Absolute ethanol, 2.5 L with catalog number 32221-2.5 L was obtained in Honeywell, Labochema.

EcoRI enzyme with catalog number ER0271 was obtained in ThermoFisher and stored at -20 °C.

EcoRI Buffer with catalog number B12 was obtained in ThermoFisher and stored at -20 °C.

SacI enzyme with catalog number ER1131 was obtained in ThermoFisher and stored at -20 °C.

SacI Buffer with catalog number B26 was obtained in ThermoFisher and stored at -20 °C.

HindIII enzyme with catalog number ER0501 was obtained in ThermoFisher and stored at -20 °C.

R buffer with catalog number BR5 was obtained in ThermoFisher and stored at -20 °C.

BamHI enzyme with catalog number ER0136S was obtained in NEB and stored at -20 °C.

r3.1 buffer with catalog number B6003S was obtained in NEB and stored at -20 °C.

2.2. Methods

2.2.1. PCR reaction

The reaction mixture was created:

Reagent	Volume/amount
5X PrimeSTAR GXL Buffer	10 µL
dNTP Mixture (2.5 mM each)	4 µL
Primer 5514 (10 µM)	1 µL
Primer 5388 (10 µM)	1 µL
Template DNA	32 ng
PrimeSTAR GXL DNA Polymerase (1.25 U/µL)	1 µL
NP NF water	Up to 50 µL

Settings for PCR:

Temperature	Time	Number of cycles
98 °C	10 s	30
60 °C	15 s	
68 °C	20 s	
4 °C	∞	1

A gel mixture of 1% agarose was created (100 mL of 1X TAE buffer, 1 g agarose, and 10 µL SYBR Safe)

Gel electrophoresis was performed at 180 V for 35 min.

2.2.2. Column purification

The PCR product was column purified using the GeneJET Gel Extraction Kit:

1. The whole volume of 50 µL of PCR product was transferred into a new 1.5 mL tube.
2. To the PCR product was added 150 µL (3 times the volume of PCR product) of Binding Buffer from the Kit. Mixed well by pipetting.
3. 200 µL (1 combined volume of PCR product and Binding Buffer) of 4 °C cold isopropanol was added to the mixture. Mixed well by pipetting.
4. The whole amount of mixture was loaded into a 2 mL column tube.
5. Span in the centrifuge 9600xg for 1 min.
6. The flowthrough was discarded.
7. The column was transferred into a new 2 mL tube.

8. 650 µL of Wash Buffer was added in the column and span in the centrifuge 9600xg for 1 min.
9. The flowthrough was discarded.
10. The column was placed in the new 2 mL tube, and span in the centrifuge 13800xg for 1 min. The flowthrough was discarded.
11. The column was transferred to the 1.5 mL tube.
12. 50 µL of NP NF Water was added to the matrix, and the tube was left for 1 min at room temperature.
13. The column was spun in the centrifuge 13800xg for 1 min.
14. The column was discarded.
15. The concentration of the PCR product was measured with Nanodrop.

2.2.3. TOPO-Blunt-II cloning

The TOPO cloning reaction mixture was prepared accordingly:

Reagent	Volume/Amount
PCR product	50-100 ng
Salt solution	1 µL
PCR-BluntII-TOPO	1 µL
NP Water	Up to 6 µL

The solution was gently mixed, spun, and left for 15 min at room temperature (27 °C).

2.2.4. Cell transformation with TOPO-Blunt-II plasmid

Antibiotic Kanamycin Sulfate was used in the experiments with TOPO plasmids.

1. 70 µL of stellar E. coli was kept in the ice box.
2. The whole volume (6 µL) of the TOPO cloning solution was added to the frozen *E.coli* and mixed without pipetting and defrizzing the cells. The cells were kept on the ice bench for 30 min.
3. Then the cells were incubated at 42 °C for 45 seconds and quickly transferred back to the ice box.
4. Carefully, while working next to an open flame, 1 mL of LB medium without antibiotics was added to the cells.
5. The cells were incubated at 37 °C for an hour, shaking at 300 rpm.
6. 500 µL of the cells were plated and spread on the plate with LB agar with an antibiotic.
7. The plate was incubated overnight (16-18 hours) at 37 °C.

2.2.5. TOPO-Blint-II plasmid typing

For plasmid typing 16 colonies were picked.

The PCR reaction mixture for plasmid typing was prepared. Calculations were made for 18 (N) tubes:

Reagent	Volume
DreamTaq Green PCR Master Mix (2X)	12.5 µL × N (225 µL)
T7 primer	0.5 µL × N (9 µL)
SP6 primer	0.5 µL × N (9 µL)
NP NF Water	11.5 µL × N (207 µL)

25 µL of the mixture was transferred into 16 PCR tubes.

While working next to the burner and using toothpick, colonies were transferred to the new Petri dish for growing, and then toothpicks were placed into the PCR tubes, and mixed thoroughly.

The PCR reaction mixture for negative control was prepared:

Reagent	Volume/Amount
DreamTaq Green PCR Master Mix (2X)	12.5 µL
Primer 5514 (10 µM)	0.5 µL
Primer 5388 (10 µM)	0.5 µL
DNA template	1 µL
NP NF Water	Up to 25 µL

The PCR program was set accordingly:

Temperature	Time	Number of cycles
95 °C	2 min	1
95 °C	30 sec	35
60 °C	30 sec	
72 °C	1 min (1 min/1 kb)	
72 °C	5 min	1
4 °C	∞	1

A gel mixture of 1% agarose was created (100 mL of 1X TAE buffer, 1 g agarose, and 10 µL SYBR Safe)

Gel electrophoresis was performed at 180 V for 40 min.

2.2.6. Overnight cultures

The whole experiment was performed in a sterile condition, using a burner.

8 colonies from the petri dish were chosen and the 10 mL tubes were marked accordingly.

Then 2 mL LB media with an appropriate antibiotic was poured into each of the 10 mL tubes.

Using a toothpick, colonies were transferred into the LB media.

Then the tubes were stored overnight at 45° angle at 37 °C, shaking at 200 rpm.

2.2.7. Preparation of the glycerol stocks and minipreps

In sterile condition, next to an open flame, in 1.5 mL tubes, 500 µL of sterile 100% glycerol and 500 µL of the overnight culture were mixed. Glycerol stocks were stored at -80 °C.

The miniprep was performed using the QIAprep Spin Miniprep Kit:

1. 1 mL of bacterial overnight culture was transferred to a 1.5 mL tube and centrifugated at 17000xg for 3 min.
2. The supernatant was discarded, and the pellet was resuspended in 250 µL of Buffer P1 by pipetting.
3. Then 250 µL of Buffer P2 was added to the mixture and mixed by inverting the tube 6 times gently (the solution turned blue); and then 350 µL of Buffer N3 was added to the mixture and immediately mixed by inverting the tube 6 times (the solution turned colourless with white cloudy flakes). Then tubes were centrifuged for 10 min at 17000xg.
4. 800 µL of the supernatant were transferred to a spin column, and the tubes were centrifugated for 1 min at 7000xg.
5. The flowthrough was discarded, and the column was transferred to a new 2 mL tube without a cup, and 650 µL of Buffer PE was added, then centrifugated for 1 min at 7000xg.
6. Once again, the flowthrough was discarded, and the column was placed in another 2 mL tube without a cap, and centrifugated for another 1 min at 7000xg.
7. The column was placed in a new 1.5 mL tube, and 50 µL of NP water was added to elute the DNA, the column was left for 1 min at room temperature, then was centrifugated for 2 min at 17000xg.
8. Concentration was measured with Nanodrop.

2.2.8. Restriction map and sequencing QC

For TOPO-Blunt-II plasmid restriction map EcoRI enzyme was used.

The mixture for the restriction map was prepared according to:

Reagent	Volume/Amount
Enzyme	1 µL
Buffer 10X	1.5 µL
Plasmid	500 ng
NP NF Water	Up to 15 µL

Setting for the restriction PCR:

Temperature	Time	Number of cycles
37 °C	1 hour	1
4 °C	∞	1

A gel mixture of 1% agarose was created (100 mL of 1X TAE buffer, 1 g agarose, and 10 µL SYBR Safe)

Gel electrophoresis was performed at 180 V for 35 min.

Samples were prepared for sequencing QC:

Reagent	Volume/Amount
Plasmid	480 ng
Primer	6 µL
NP NF Water	Up to 17 µL

Plasmids were sent to the Microsynth company for Sangar sequencing. Results were analyzed with Sequencher 5.4.6. software.

2.2.9. 2-step PCR and column purification

The reaction mixture was created:

Reagent	Volume/Amount
5X PrimeSTAR GXL Buffer	10 µL
dNTP Mixture	4 µL
Primer 5514 (10 µM)	1 µL
Primer 5388 (10 µM)	1 µL
TOPO plasmid	8 ng

PrimeSTAR GXL DNA Polymerase	1 µL
NP NF water	Up to 50 µL

Settings for 2-step GXL PCR:

Temperature	Time	Number of cycles
98 °C	10 s	3
60 °C	15 s	
68 °C	10 s/1 kb (12 s)	
98 °C	10 s	27
68 °C	10 s/1 kb (12 s)	
4 °C	∞	1

A gel mixture of 1% agarose was created (100 mL of 1X TAE buffer, 1 g agarose, and 10 µL SYBR Safe)

Gel electrophoresis was performed at 180 V for 40 min.

PCR products were column purified as it is described in 2.2.2. chapter.

2.2.10. Gibson Assembly (GA)

The donor backbone was digested with EcoRI enzyme and column purified. Concentration was measured with Nanodrop. C=59.3 ng/µL.

Gibson calculator was used to calculate the volume of reagents.

The mixture was prepared according to:

Product	S050 (c=63.3 ng/µL)	S051 (c=47.2 ng/µL)	S052 (c=21.1 ng/µL)	S053 (c=13.7 ng/µL)
GAMM 2X	5 µl	5 µl	5 µl	5 µl
Backbone	2.59 µl	2.59 µl	2.59 µl	2.59 µl
PCR product	1.03 µl (diluted 3 times)	1.36 µl (diluted 3 times)	1.16 µl	1.8 µl
NP NF Water	1.38 µl (up to 10 µl)	1.05 µl (up to 10 µl)	1.25 µl (up to 10 µl)	0.61 µl (up to 10 µl)

The mixtures were kept at 50 °C for 20 min.

2.2.11. Cell transformation with Gibson Assembly

5 µL of GA mixture was used for cell transformation.

Antibiotic carbenicillin was used in the experiments with GA plasmids.

Cell transformation was performed as described in 2.2.4. chapter.

2.2.12. GA plasmid typing

The PCR reaction mixture for plasmid typing was prepared. Calculations were made for 34 (N) tubes:

Reagent	Volume
DreamTaq Green PCR Master Mix (2X)	12.5 µL × N (425 µL)
5605 primer (10 µM)	0.5 µL × N (17 µL)
5534 primer (10 µM)	0.5 µL × N (17 µL)
NP NF Water	11.5 µL × N (391 µL)

25 µL of the mixture was transferred into 32 PCR tubes.

While working next to the burner and using toothpick, colonies were transferred to the new Petri dish for growing, and then toothpicks were placed into the PCR tubes, and mixed thoroughly. 2 PCR tubes were left without a DNA template for negative control.

The PCR program was set accordingly:

Temperature	Time	Number of cycles
95 °C	2 min	1
95 °C	30 sec	35
60 °C	30 sec	
72 °C	1 min (1 min/1 kb)	
72 °C	5 min	1
4 °C	∞	1

A gel mixture of 2% agarose was created (100 mL of 1X TAE buffer, 1 g agarose, and 10 µL SYBR Safe)

Gel electrophoresis was performed at 180 V for 40 min.

2.2.13. Overnight cultures, glycerol stocks, and minipreps

Overnight cultures were made as described in 2.2.6. chapter.

Glycerol stocks and minipreps were made as described in 2.2.7. chapter.

2.2.14. Restriction map and sequencing QC

For the restriction map of GA plasmids S051, S052, and S053 SacI enzyme was used.

For the restriction map of GA plasmid S050 PvuII enzyme was used.

Restriction map and sequencing QC were performed as described in 2.2.8. chapter.

2.2.14. Maxipreps

Overnight culture was prepared using an open flame. 40 µL of glycerol stock of each sample was added to 4 different bottles with 200 mL of LB broth and 200 µL of carbenicillin. Culture was incubated at 37 °C, shaking at 180 rpm for 16 h.

Maxipreps were prepared using the HiSpeed Plasmid Maxi Kit:

1. 200 mL of overnight culture was centrifugated at 3500 rpm for 20 min.
2. The supernatant was removed and the pellet was resuspended homogeneously in 10 mL of BufferP1.
3. 10 mL of Buffer P2 was added and mixed by inverting the tube 4-6 times. The tube was incubated for 5 min at room temperature.
4. 10 mL of pre-chilled Buffer P3 was added and mixed by inverting 4-6 times, and the tube was centrifugated at 2000 rpm for 10 min.
5. HiSpeed Tip was equilibrated with 10 mL Buffer QBT, allowing it to enter the resin. It was left to completely drip out.
6. Lysate was poured into the barrel of the QIAfilter Cartridge and incubated at room temperature for 10 min. The cap from the QIAfilter Cartridge outlet nozzle was removed, and the cell lysate was filtered by gently inserting the plunger into the QIAfilter Cartridge into the equilibrated HiSpeed Tip. It was left to completely drip out.
7. After the lysate had entered, the HiSpeed Tip was washed with 60 mL Buffer QC and was left to completely drip out.
8. DNA was eluted with 15 mL Buffer QF into a 50 mL tube.
9. DNA was precipitated by adding 10.5 mL of isopropanol, mixed, and incubated for 5 min.
10. During the incubation, the plunger from a 30 mL syringe was removed, and the QIAprecipitator Module was attached to the outlet nozzle.
11. The QIAprecipitator was placed over a waste bottle, and the eluate-isopropanol mixture was transferred into the syringe and filtered through the QIAprecipitator using constant pressure from the plunger.
12. The QIAprecipitator was removed from the syringe, and the plunger was pulled out. The QIAprecipitator was reattached, and 2 mL of 70% ethanol was added to the

syringe. DNA was washed by inserting the plunger and pressing the ethanol through the QIAprecipitator.

13. The QIAprecipitator was removed from the syringe, and the plunger was pulled out. The QIAprecipitator was attached again, the plunger was inserted, and the membrane was dried by pressing air through the QIAprecipitator forcefully. This step was repeated 7 times.
14. The outlet nozzle of the QIAprecipitator was dried with absorbent paper.
15. The plunger from a new 5 mL syringe was removed, the QIAprecipitator was attached to the syringe, and the outlet was held over a 1.5 mL collection tube. 500 µL of NF NP water was added to the 5 mL syringe, and the DNA was eluted into the collection tube using constant pressure from the plunger.
16. The QIAprecipitator was removed from the 5 mL syringe, the plunger pulled out, and the QIAprecipitator was reattached to the 5 mL syringe.
17. The eluate from step 18 was transferred to the 5 mL syringe and eluted for a second time into the same 1.5 mL tube.
18. Concentration was measured with Nanodrop.

2.2.15. Thawing and expansion of the cell culture

1. Cell culture was retrieved from the liquid nitrogen. And kept in the hand for 5 min, allowing the cell culture to partly thaw.
2. 1 mL of cell culture media was added to the 1 mL of thawed cell culture, and 2 mL of the entire volume was transferred without pipetting into a 15 mL tube.
3. The tube was centrifuged at 300xg for 3 min.
4. The supernatant was removed.
5. The pellet was resuspended in 5 mL of media and transferred to the cell culture flask. 15 mL of media was added to the flask, allowing cells to grow.
6. The flask was transferred to the incubator with 37 °C and 5% CO2 settings.

To maintain the thawed cell culture, cell culture should be checked every day, and media should be added if necessary. Cell culture media should be changed once per 2 or 3 days.

2.2.16. Electroporating the cells

To knock-in reporters into the cancer cells 3 µg of DNA plasmid and 1 µg of Cas9 plasmid. The volume of the DNA mixture should exceed 10 µL per 10^6 electroporated cells.

1. The media was removed from cell culture.
2. The cell culture was washed with PBS.

3. 3 mL of 0.5X accutase was added to the cells. Cells were left to detach for about 3 min.
4. Accutase was removed, and 5 mL of PBS was added to the cells.
5. Then 10 mL of cell culture media was added, and the cells were transferred into the 15 mL tube.
6. The tube was centrifugated at 300xg for 3 min. The supernatant was removed.
7. The cell pellet was resuspended in the media. Cells were counted using Countess. (To count the cells in a 1.5 mL tube cells were mixed with Trypan blue dye at a 1:1 ratio, and 15 µl of this mix was applied onto the Countess chamber and inserted into the Countess.)
8. Cells were centrifugated again at 300xg for 3 min. The supernatant was removed.
9. The pellet was resuspended in the Optim-MEM at a ratio of 100 µL per 10^6 cells.
10. 10^6 cells were transferred into a separate tube and a mixture of DNA plasmids and Cas9 plasmid was added into the cells.
11. The mixture was transferred into the electroporation cuvette.
12. A new flask with media and a pipette with 1 mL of media were pre-prepared.
13. Electroporation cuvette was inserted into the cuvette chamber.
14. After electroporation was done, the cuvette was ejected from the cuvette chamber, and 1 mL of the media was quickly added to the cells.
15. Media with electroporated cells were transferred into the pre-prepared flask with media.
16. The cell culture flask was transferred into the incubator with 37 °C and 5% CO2 settings, allowing the cells to recover and grow.

3. RESULTS

3.1. Topo-Blunt-II cloning.

DNA gBlocks were created using the MTn sequence from Jiang et al., 2020 paper. KDEL, COX8A, and CD proteins sequences were used. Sequences were created using the UniProt website and ApE software.

The ends of the gBlocks were trimmed using PCR to create blunt-end double-strained sequences and then they were column purified. The concentration of the PCR products was measured with Nanodrop and are listed in the table below:

PCR product	Concentration
S050-COX8A-MTn	36.8 ng/µL
S051-KDEL-MTn	76.1 ng/µL
S052-MTn-CD8	72.6 ng/µL
S053-CD8-MTn	65.7 ng/µL

Blunt PCR products were used for TOPO-Blunt-II cloning. TOPO-Blunt-II cloning and cell transformation were performed according to the protocol. The cloning mixture was transformed into stellar competent *E.coli* cells.

3.2. Plasmid typing. Restriction map.

16 colonies of S050-COX8A-MTn TOPO plasmid were chosen for plasmid typing with T7 and SP6 primers.

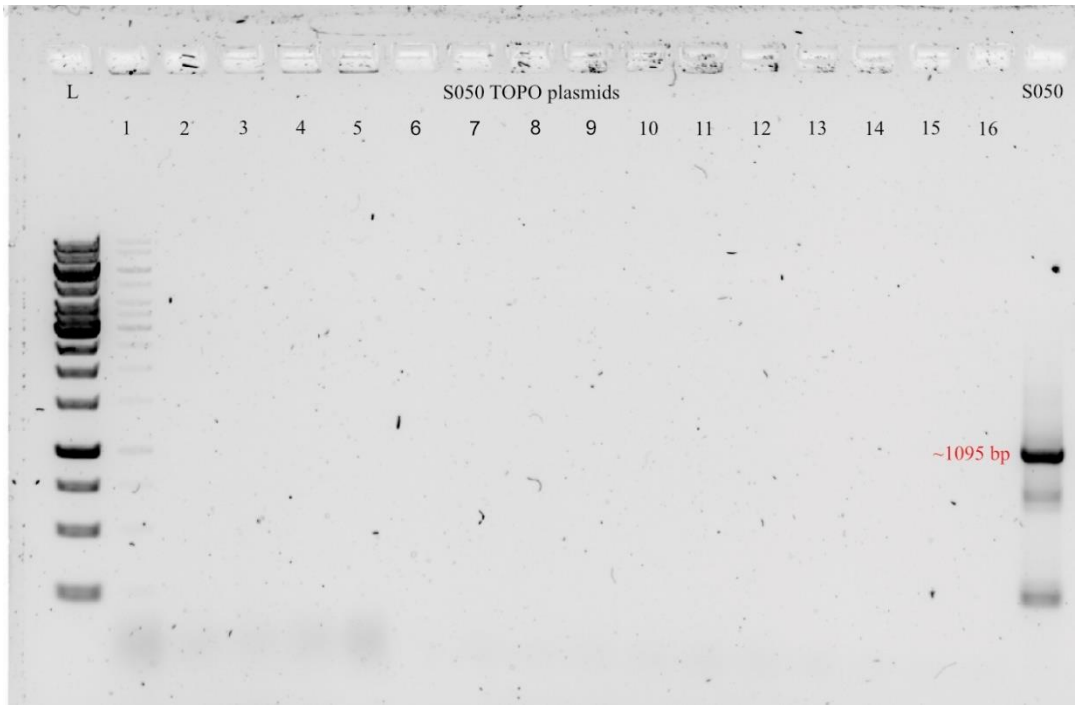

Figure 3.1. Gel electrophoresis of the S050-COX8A-MTn TOPO-Blunt-II plasmid typing. L – a 1 kb gene ruler; under numbers 1-16 numbers there were 16 clones of S050 plasmids. Under S050 there was a product of PCR of gBlock S050-COX8A-MTn, as a control.

As it is shown in figure 3.1 TOPO-Blunt-II plasmid typing did not show any bands, meaning that the reaction did not work. A possible reason for this could be the problem with the ordered primers.

TOPO-Blunt-II backbone has a kanamycin antibiotic resistance, and on the LB plate with kanamycin grew more than 16 colonies, which could mean that there were TOPO backbones in the *E.coli* cells. Assuming that, glycerol stocks and minipreps were made from 7 of these clones, and then restriction map with EcoRI enzyme was performed.

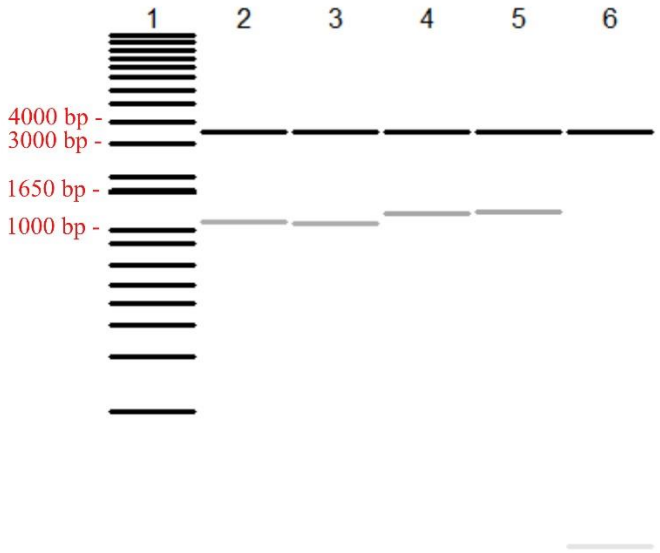

Figure 3.2. In silico restriction map with EcoRI enzyme with TOPO plasmids. 1 – 1 kb plus gene ruler. There were S050-COX8A-MTn, S051-KDEL-MTn, S052-MTn-CD8, and S053-CD8-MTn on the 2, 3, 4, and 5 columns respectively. On the 6 column, there was TOPO-Blunt-II backbone.

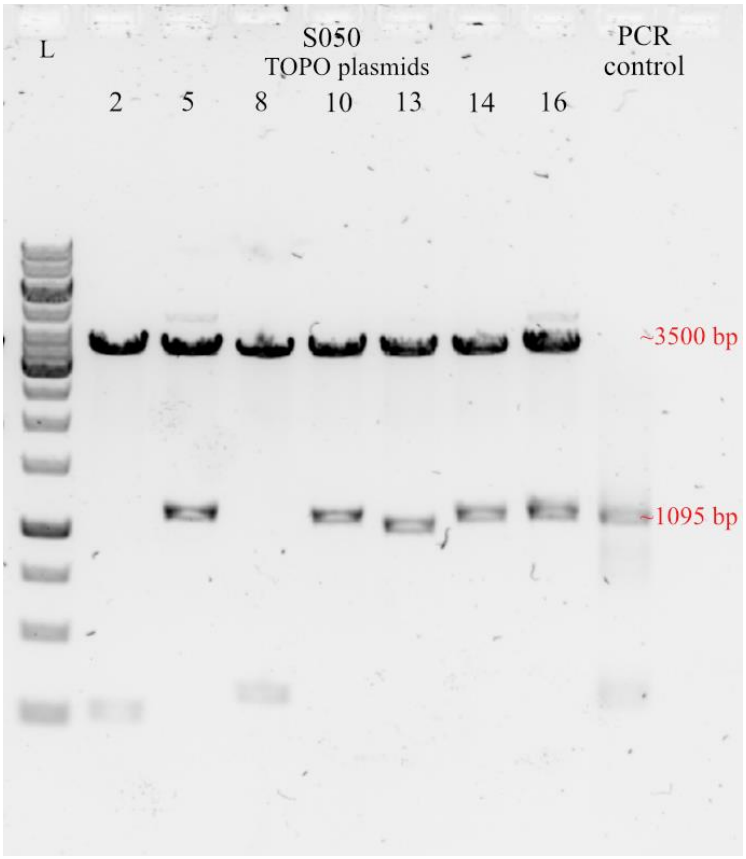

Figure 3.3. Restriction map with EcoRI enzyme of the 7 colonies S050-COX8A-MTn. L – a 1 kb gene ruler; PCR product is used as a control.

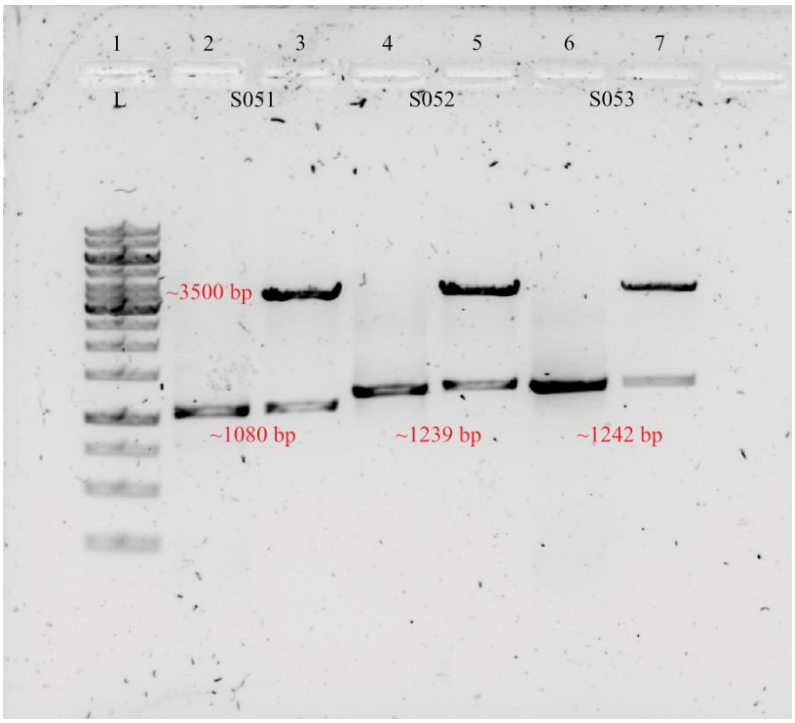

Figure 3.4. Restriction map with EcoRI enzyme S051-KDEL-MTn, S052-MTn-CD8, and S053-CD8-MTn. L – a 1 kb gene ruler; PCR products of plasmid were used as a control; in the 2, 4, and 6 columns there were PCR products, and in the 3, 5, and 7 columns there were TOPO plasmids.

In figure 3.2 is shown the expected restriction map of TOPO-Blunt-II plasmids with EcoRI enzyme. TOPO backbone is around 3500 bp, whereas S050-COX8A-MTn is 1095 bp, S051-KDEL-MTn is 1080 bp, S052-MTn-CD8 is 1239 bp, and S053-CD8-MTn is 1242 bp.

In figure 3.3 and figure 3.4, there are results of gel electrophoresis of TOPO plasmids. Out of 7 clones of S050-COX8A-MTn 5 had an insert similar to the expected length 1095 bp and PCR product. TOPO clones of S051-KDEL-MTn, S052-MTn-CD8, and S053-CD8-MTn had inserts with similar to the PCR products and expected length.

Clones that showed bands of expected length were chosen and sent for quality control sequencing – Sangar sequencing in the Microsynth company. Results were analyzed with Sequencher software. Samples with no mutation in them were chosen for further experiments.

Concentrations of the chosen TOPO plasmids were measured with Nanodrop and are listed below:

TOPO plasmid	Concentration
S050-COX8A-MTn	368.5 ng/µL
S051-KDEL-MTn	159.7 ng/µL
S052-MTn-CD8	176.2 ng/µL
S053-CD8-MTn	292.4 ng/µL

3.3. 2-step PCR. Gibson Assembly.

1005CHA donor was used as a backbone for Gibson Assembly (GA). The donor backbone was fully digested with EcoRI enzyme to cut the EGFP, 732 bp, out. The donor plasmid, 7760 bp, was then column purified to eliminate salts from the digestion reaction. Concentration was measured with Nanodrop, c=59.3 ng/µL. The donor backbone was prepared by Khushboo Shah.

In order to perform GA with the 1005CHA donor 2-step PCR with the chosen plasmids was performed, and PCR products were column purified. 2-step PCR results were analyzed with gel electrophoresis, as shown in figure 3.5.

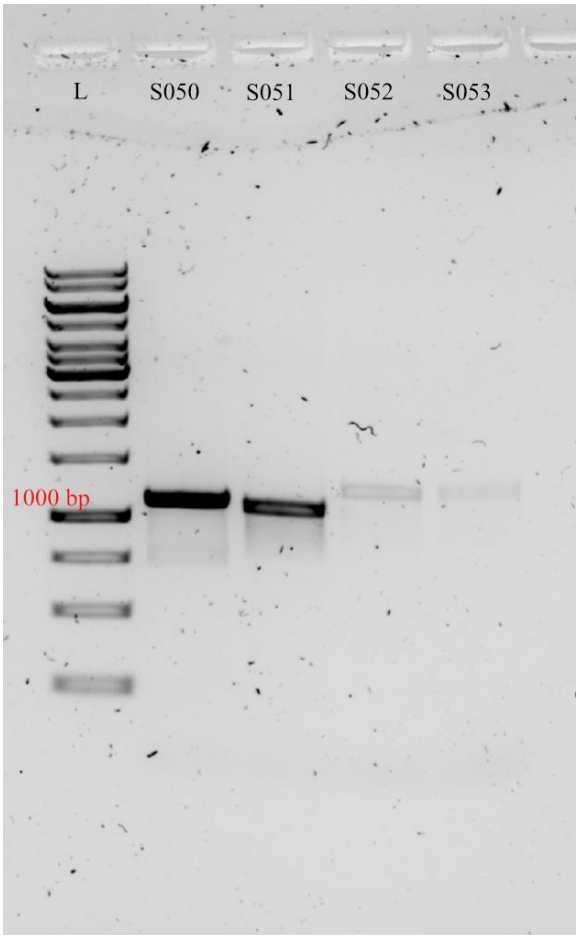

Figure 3.5. 2-step PCR results of the chosen clones of TOPO plasmids. L – 1 kb gene ruler. PCR products showed a band around 1000-1200 bp.

Concentrations of the 2-step PCR products were measured with Nanodrop and are listed below:

2-step PCR product	Concentration
S050-COX8A-MTn	63.3 ng/µL
S051-KDEL-MTn	47.2 ng/µL
S052-MTn-CD8	21.1 ng/µL
S053-CD8-MTn	13.7 ng/µL

GA and cell transformation were performed according to the protocol, and 5 µL of the mixture was transformed into stellar competent *E.coli* cells.

3.4. Plasmid typing. Restriction map.

7 colonies of S050-COX8A-MTn and S052-MTn-CD8 and 8 colonies of S051-KDEL-MTn and S053-CD8-MTn were picked for the plasmid typing. Primers for plasmid typing were chosen to create 127 bp bands. A mixture for plasmid typing without a sample was used as a negative control.

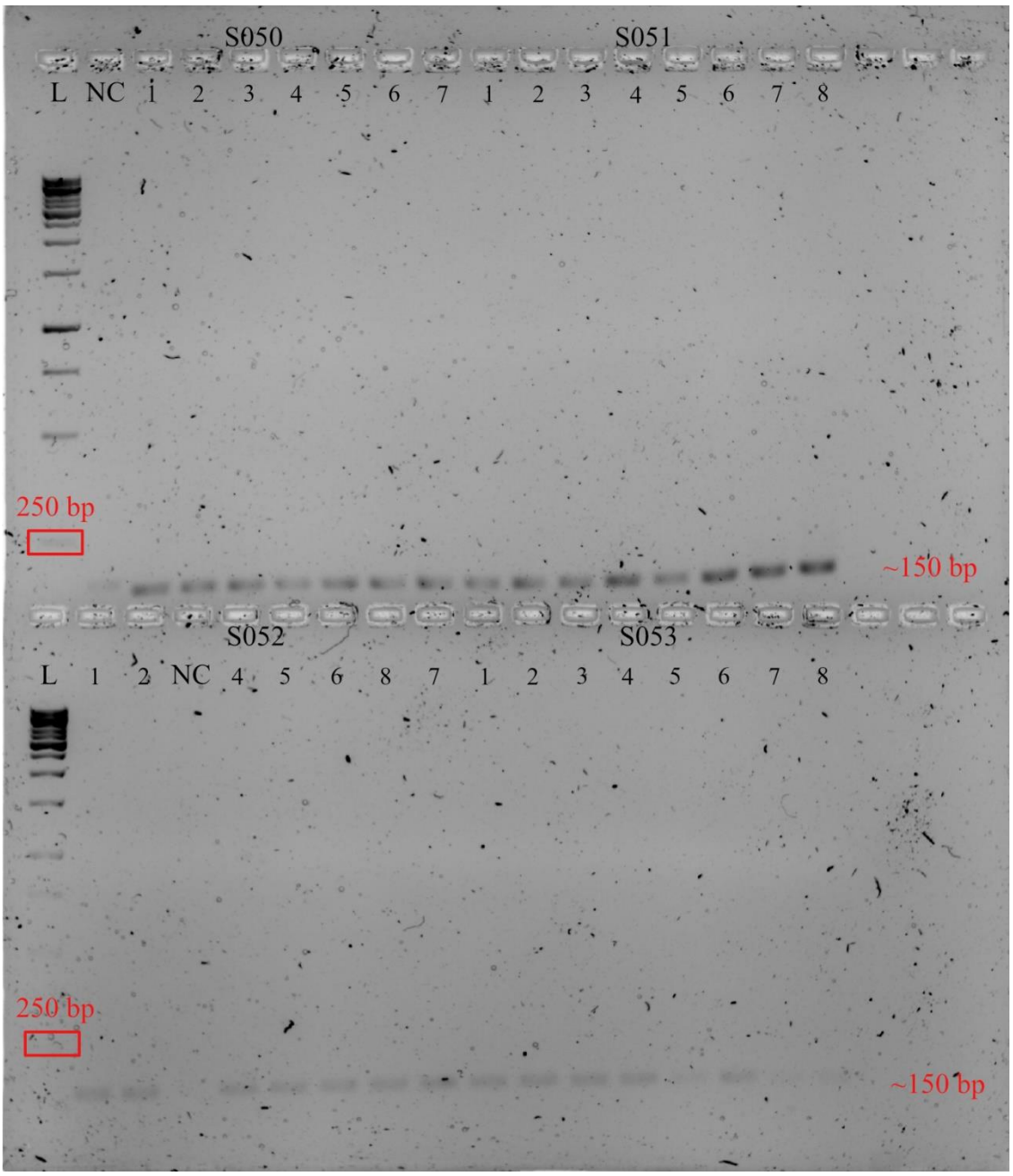

Figure 3.6. 2% agarose gel electrophoresis of GA plasmid typing of S050-COX8A-MTn, S052-MTn-CD8, S051-KDEL-MTn, and S053-CD8-MTn. L – 1 kb gene ruler; NC – negative control.

As is shown in figure 3.6. plasmid typing gave bands with approximately 130 bp length in each clone of each sample. This meant that there were expected inserts in all of the picked colonies. Therefore, three colonies of each sample were picked for glycerol stocks and minipreps.

Figure 3.7. In silico restriction map of GA plasmid of S050-COX8A-MTn with PvuII enzyme. 1 – 1 kb plus gene ruler. 2 – GA plasmid itself, 3 – GA backbone without any insert.

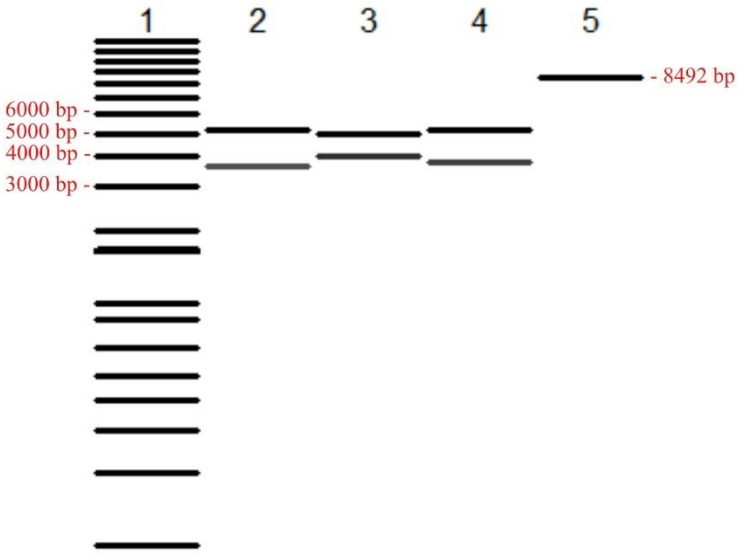

Figure 3.8. In silico restriction map of GA plasmid with SacI enzyme. 1 – 1 kb plus gene ruler. S051-KDEL-MTn, S052-MTn-CD8, and S053-CD8-MTn GA plasmids were on the 2, 3, and 4 respectively. On the 5 column, there was a GA backbone without any insert.

To double-check that there were expected inserts in the clones, a restriction map was performed. Clones of S051-KDEL-MTn, S052-MTn-CD8, and S053-CD8-MTn were digested with SacI enzyme. S050-COX8A-MTn was digested with the PvuII enzyme. As shown in figure 3.7 GA plasmid with S050-COX8A-MTn insert should give 5 bands with 4365 bp, 2513 bp, 1600 bp,

274 bp, and 69 bp, whereas GA backbone without an insert should give 2 bands 5979 bp and 2513 bp.

As shown in figure 3.8 GA plasmid with S051-KDEL-MTn, S052-MTn-CD8, and S053-CD8-MTn after digestion with SacI enzyme should give 2 bands, one should be around 5000 bp and another should be from 3500 bp to 4000 bp, whereas GA backbone should give only 1 band with 8492 bp length.

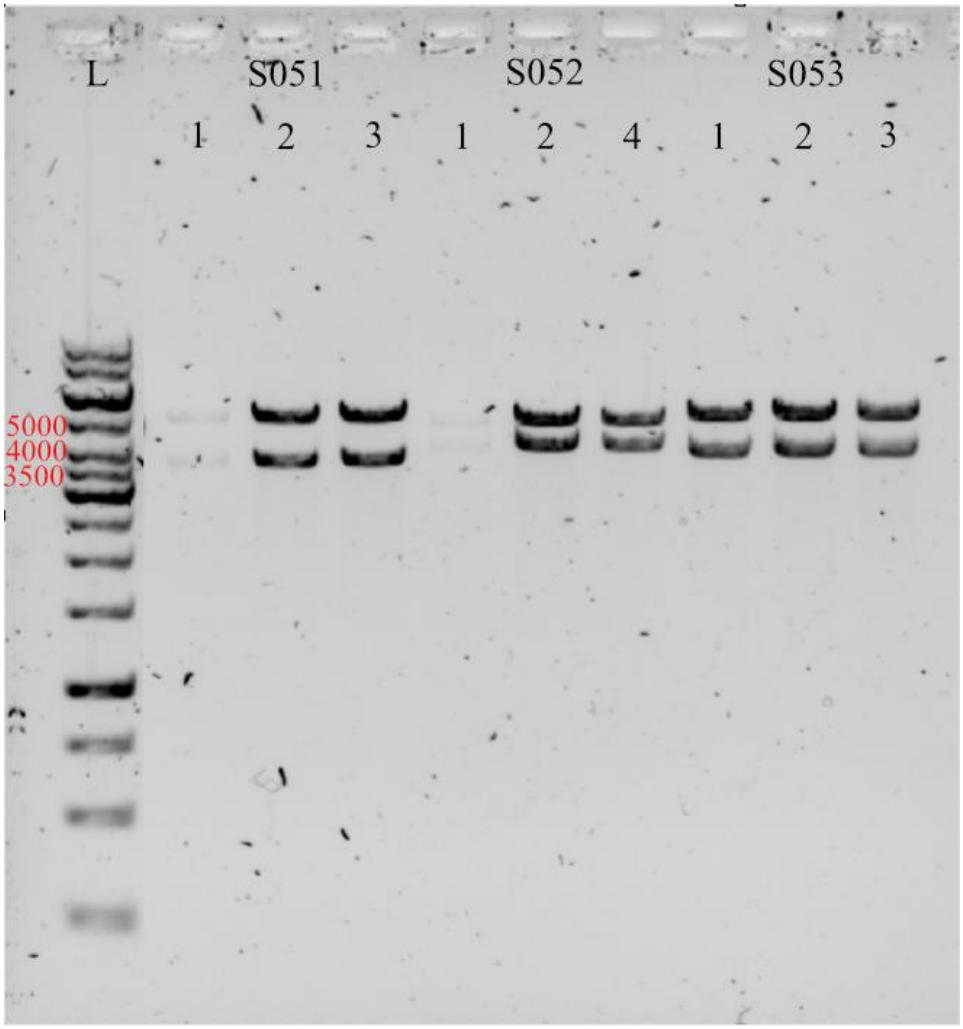

Figure 3.9. Gel electrophoresis of a restriction map with SacI enzyme of S051-KDEL-MTn, S052-MTn-CD8, and S053-CD8-MTn. L – 1 kb gene ruler.

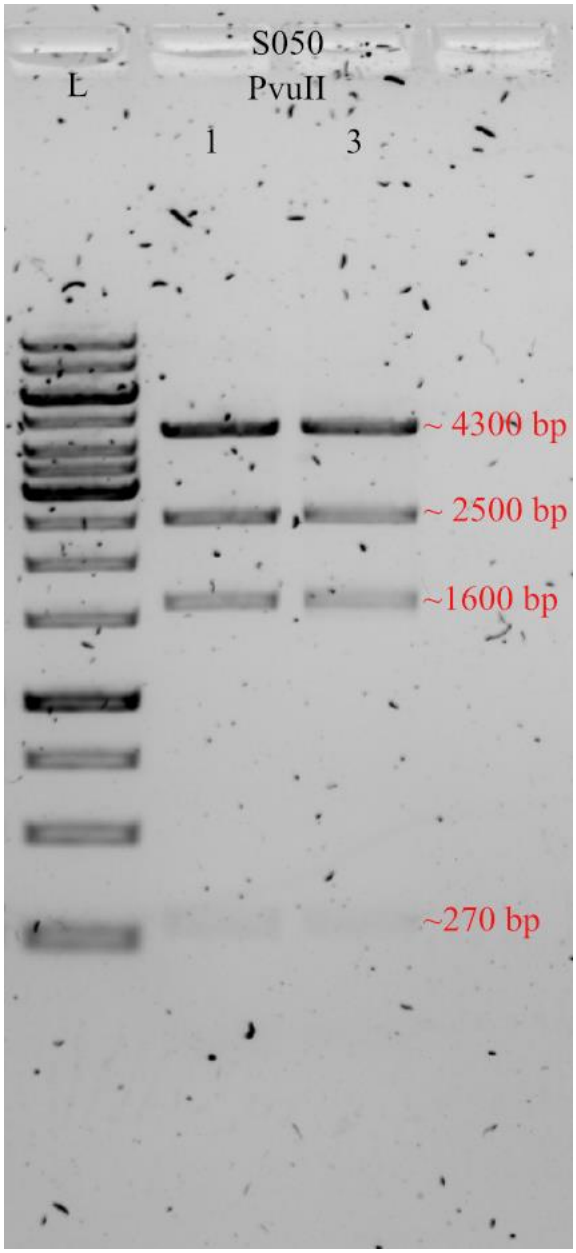

Figure 3.10. Gel electrophoresis of a restriction map with PvuII enzyme of S050-COX8A-MTn. L – 1 kb gene ruler.

As shown in figure 3.9 each of the clones of S051-KDEL-MTn, S052-MTn-CD8, and S053-CD8-MTn after digestion with SacI enzyme showed 2 bands around an expected length of 5000 bp and another from 3500 bp to 4000 bp. As shown in figure 3.10 both clones of S050-COX8A-MTn showed 4 bands of expected length around 4300 bp, 2500 bp, 1600 bp, and 270 bp. It is possible to assume that the 5th band, which was supposed to be around 70 bp is too small to be seen in the gel electrophoresis.

2 clones of each GA plasmid with clear results from the restriction map were sent for Sangar sequencing in the Microsynth company. Clones with no mutations were chosen for maxiprep to have plasmids ready for electroporation into the cells.

3.5. Minipreps and Maxipreps of the GA plasmids.

The concentrations of the chosen GA plasmids for the maxipreps are listed below:

GA plasmid in miniprep	Concentration
S050-COX8A-MTn	157.5 ng/µL
S051-KDEL-MTn	98.3 ng/µL
S052-MTn-CD8	82.1 ng/µL
S053-CD8-MTn	56.4 ng/µL

Maxipreps were performed according to the protocol from the glycerol stocks of the chosen clones. Concentrations were measured with Nanodrop and are listed below;

GA plasmid in maxiprep	Concentration
S050-COX8A-MTn	69.4 ng/µL
S051-KDEL-MTn	77.6 ng/µL
S052-MTn-CD8	112.7 ng/µL
S053-CD8-MTn	3.2 ng/µL

The molecular weight of the maxipreps could be calculated according to formula 500 µL × concentration. Therefore, S050-COX8A-MTn, S051-KDEL-MTn, S052-MTn-CD8, and S053-CD8-MTn maxipreps weight was 34.7 µg, 38.8 µg, 56.35 µg, and 1.6 µg.

Maxipreps were stored at -20 °C.

4. DISCUSSION

EM imaging of POIs in human cells can give more valuable information for understanding cell biology, drug, and disease development.

During the laboratory work, EM sensors for mitochondria, ER, and inner and outer membranes of the cell culture in human cells were prepared, synthesized and cloned. GA plasmids were created with 1005CHA donor backbone and checked for mutation with Sangar sequencing.GA plasmids showed no mutations with the targeted sequence, and they were cloned using competent stellar *E. coli* cells. The concentration of minipreps of the EM reporters S050-COX8A-MTn, S051-KDEL-MTn, S052-MTn-CD8, and S053-CD8-MTn were 157.5 ng/µL, 98.3 ng/µL, 82.1 ng/µL, and 56.4 ng/µL respectively.

Maxiprep of all 4 GA plasmids were prepared, and the concentration of S050-COX8A-MTn, S051-KDEL-MTn, S052-MTn-CD8, and S053-CD8-MTn were 69.4 ng/µL, 77.6 ng/µL, 112.7 ng/µL, and 3.2 ng/µL respectively. Obtained concentrations (c) of the S050-COX8A-MTn, S051-KDEL-MTn, and S052-MTn-CD8 plasmids allow to proceed with electroporation into the human cells. The required weight of the DNA plasmid for electroporation is 3 µg per 10^6 electroporated cells (see chapter 2.2.16), and the weight of the S050-COX8A-MTn, S051-KDEL-MTn, and S052-MTn-CD8 plasmids are 34.7 µg, 38.8 µg, and 56.35 µg, respectively.

Maxiprep for the inner cellular membrane, S053-CD8-MTn, had a low concentration, making it unable to proceed with the electroporation step. This most likely has happened due to the mistakes in the Maxiprep procedure, such as alkaline lysis being inefficient or insufficient volume of lysis being used (QIAGEN Plasmid Purification Handbook, 2023).

Therefore, EM sensors for mitochondria, ER, and outer cellular membrane in human cells could be electroporated into compatible cell cultures (Alghadban et al., 2020; Wardyn et al., 2021). Then, cell culture could be revived with appropriate conditions, and checked with flow cytometry (Bajgelman, 2019; Sherba et al., 2020). Cells that contain EM sensors should give a fluorescent signal because EM reporters contain GFP in their sequence.

CONCLUSIONS

DONOR plasmids with EM reporters for localization of the POIs in the human cells were successfully cloned using Gibson Assembly, and quality controlled with Sangar sequencing and gel electrophoresis.

DONOR plasmids with EM reporters for mitochondria (Mch), EM, and inner and outer cellular membrane (OCM) were successfully isolated. DONOR plasmids with Mch, EM, and OCM EM reporters were prepared for the electroporation onto compatible cell culture.

DESCRIPTION OF PERSONAL INPUT

I created and cloned EM reporters for visualization of human cell organelles.

I analyzed the gel electrophoresis and sequencing results.

I performed all the executed experiments in the research project, analyzed their results, and made the conclusions, including analysis of the Sangar sequencing results.

I analyzed literature related to the research area.

AKNOWLEDGMENTS

I thank my supervisor, PhD. Dr. Jonathan Lee Arias Fuenzalida, for project planning, creating the sequences for EM reporters, troubleshooting the results, his support throughout my master's thesis work, and writing review.

I thank Khushboo Shah for her help with the 1005CHA donor backbone.

LIST OF REFERENCES

Adan, A., Alizada, G., Kiraz, Y., Baran, Y., & Nalbant, A. (2017). Flow cytometry: Basic principles and applications. *Critical Reviews in Biotechnology*, *37*(2), 163–176. https://doi.org/10.3109/07388551.2015.1128876

Alexopoulou, A. N., Couchman, J. R., & Whiteford, J. R. (2008). The CMV early enhancer/chicken β actin (CAG) promoter can be used to drive transgene expression during the differentiation of murine embryonic stem cells into vascular progenitors. *BMC Cell Biology*, *9*, 2. https://doi.org/10.1186/1471-2121-9-2

Alghadban, S., Bouchareb, A., Hinch, R., Hernandez-Pliego, P., Biggs, D., Preece, C., & Davies, B. (2020). Electroporation and genetic supply of Cas9 increase the generation efficiency of CRISPR/Cas9 knock-in alleles in C57BL/6J mouse zygotes. *Scientific Reports*, *10*(1), 17912. https://doi.org/10.1038/s41598-020-74960-7

Arias-Fuenzalida, J., Jarazo, J., Qing, X., Walter, J., Gomez-Giro, G., Nickels, S. L., Zaehres, H., Schöler, H. R., & Schwamborn, J. C. (2017). FACS-Assisted CRISPR-Cas9 Genome Editing Facilitates Parkinson's Disease Modeling. *Stem Cell Reports*, *9*(5), 1423–1431. https://doi.org/10.1016/j.stemcr.2017.08.026

Bajgelman, M. C. (2019). Chapter 8—Principles and applications of flow cytometry. In G. Misra (Ed.), *Data Processing Handbook for Complex Biological Data Sources* (pp. 119–124). Academic Press. https://doi.org/10.1016/B978-0-12-816548-5.00008-3

Banan, M. (2020). Recent advances in CRISPR/Cas9-mediated knock-ins in mammalian cells. *Journal of Biotechnology*, *308*, 1–9. https://doi.org/10.1016/j.jbiotec.2019.11.010

Barman, A., Deb, B., & Chakraborty, S. (2020). A glance at genome editing with CRISPR–Cas9 technology. *Current Genetics*, *66*(3), 447–462. https://doi.org/10.1007/s00294-019-01040-3

Blair, T. A., Frelinger, A. L., & Michelson, A. D. (2019). 35—Flow Cytometry. In A. D. Michelson (Ed.), *Platelets (Fourth Edition)* (pp. 627–651). Academic Press. https://doi.org/10.1016/B978-0-12-813456-6.00035-7

Bordat, A., Houvenaghel, M.-C., & German-Retana, S. (2015). Gibson assembly: An easy way to clone potyviral full-length infectious cDNA clones expressing an ectopic VPg. *Virology Journal*, *12*(1), 89. https://doi.org/10.1186/s12985-015-0315-3

Brischigliaro, M., & Zeviani, M. (2021). Cytochrome *c* oxidase deficiency. *Biochimica et Biophysica Acta (BBA) - Bioenergetics*, *1862*(1), 148335. https://doi.org/10.1016/j.bbabio.2020.148335

Brust, M., Walker, M., Bethell, D., Schiffrin, D. J., & Whyman, R. (1994). Synthesis of thiol-derivatised gold nanoparticles in a two-phase Liquid–Liquid system. *Journal of the Chemical Society, Chemical Communications*, *7*, 801–802. https://doi.org/10.1039/C39940000801

Brzezinski, P., Moe, A., & Ädelroth, P. (2021). Structure and Mechanism of Respiratory III–IV Supercomplexes in Bioenergetic Membranes. *Chemical Reviews*, *121*(15), 9644–9673. https://doi.org/10.1021/acs.chemrev.1c00140

Choi, S.-Y., Ro, H., & Yi, H. (2019). Methods That Make Your Cloning Life Easier. In S.-Y. Choi, H. Ro, & H. Yi (Eds.), *DNA Cloning: A Hands-on Approach* (pp. 99–121). Springer Netherlands. https://doi.org/10.1007/978-94-024-1662-6_6

Davis, A. J., & Chen, D. J. (2013). DNA double strand break repair via non-homologous end-joining. *Translational Cancer Research*, *2*(3), 130–143. https://doi.org/10.3978/j.issn.2218-676X.2013.04.02

Diestra, E., Fontana, J., Guichard, P., Marco, S., & Risco, C. (2009). Visualization of proteins in intact cells with a clonable tag for electron microscopy. *Journal of Structural Biology*, *165*(3), 157–168. https://doi.org/10.1016/j.jsb.2008.11.009

Esensten, J. H., Helou, Y. A., Chopra, G., Weiss, A., & Bluestone, J. A. (2016). CD28 costimulation: From mechanism to therapy. *Immunity*, *44*(5), 973–988. https://doi.org/10.1016/j.immuni.2016.04.020

Gerondopoulos, A., Bräuer, P., Sobajima, T., Wu, Z., Parker, J. L., Biggin, P. C., Barr, F. A., & Newstead, S. (2021). A signal capture and proofreading mechanism for the KDEL-receptor explains selectivity and dynamic range in ER retrieval. *eLife*, *10*, e68380. https://doi.org/10.7554/eLife.68380

Gibson, D. G., Young, L., Chuang, R.-Y., Venter, J. C., Hutchison, C. A., & Smith, H. O. (2009). Enzymatic assembly of DNA molecules up to several hundred kilobases. *Nature Methods*, *6*(5), 343–345. https://doi.org/10.1038/nmeth.1318

Gould, S. I. (2024). Prime editing sensors enable multiplexed genome editing. *Nature Reviews Genetics*, 1–1. https://doi.org/10.1038/s41576-024-00737-7

Green, M. R., & Sambrook, J. (2019). Analysis of DNA by Agarose Gel Electrophoresis. *Cold Spring Harbor Protocols*, *2019*(1), pdb.top100388. https://doi.org/10.1101/pdb.top100388

Gruh, I., Wunderlich, S., Winkler, M., Schwanke, K., Heinke, J., Blömer, U., Ruhparwar, A., Rohde, B., Li, R.-K., Haverich, A., & Martin, U. (2008). Human CMV immediate-early enhancer: A useful tool to enhance cell-type-specific expression from lentiviral vectors. *The Journal of Gene Medicine*, *10*(1), 21–32. https://doi.org/10.1002/jgm.1122

Gulati, N. M., Torian, U., Gallagher, J. R., & Harris, A. K. (2019). Immunoelectron Microscopy of Viral Antigens. *Current Protocols in Microbiology*, *53*(1), e86. https://doi.org/10.1002/cpmc.86

Hassona, M. M., Radwan, E. M., Abdelsameea, E., Estaphan, S., Abd Elrhman, H. E., Abdel-Samiee, M., & Naguib, M. (2021). The Putative Role of Natural Killer Cells in Patients with Hepatitis C Virus-Related Hepatocellular Carcinoma. *Asian Pacific Journal of Cancer Prevention : APJCP*, *22*(8), 2559–2567. https://doi.org/10.31557/APJCP.2021.22.8.2559

Hockemeyer, D., & Jaenisch, R. (2016). Induced Pluripotent Stem Cells Meet Genome Editing. *Cell Stem Cell*, *18*(5), 573–586. https://doi.org/10.1016/j.stem.2016.04.013

Iwamoto, M., Mori, C., Hiraoka, Y., & Haraguchi, T. (2014). Puromycin resistance gene as an effective selection marker for ciliate Tetrahymena. *Gene*, *534*(2), 249–255. https://doi.org/10.1016/j.gene.2013.10.049

Janik, E., Niemcewicz, M., Ceremuga, M., Krzowski, L., Saluk-Bijak, J., & Bijak, M. (2020). Various Aspects of a Gene Editing System—CRISPR–Cas9. *International Journal of Molecular Sciences*, *21*(24), Article 24. https://doi.org/10.3390/ijms21249604

Jiang, Z., Jin, X., Li, Y., Liu, S., Liu, X.-M., Wang, Y.-Y., Zhao, P., Cai, X., Liu, Y., Tang, Y., Sun, X., Liu, Y., Hu, Y., Li, M., Cai, G., Qi, X., Chen, S., Du, L.-L., & He, W. (2020). Genetically encoded tags for direct synthesis of EM-visible gold nanoparticles in cells. *Nature Methods*, *17*(9), 937–946. https://doi.org/10.1038/s41592-020-0911-z

Kalina, T., Fišer, K., Pérez-Andrés, M., Kuzílková, D., Cuenca, M., Bartol, S. J. W., Blanco, E., Engel, P., & van Zelm, M. C. (2019). CD Maps—Dynamic Profiling of CD1–CD100 Surface Expression on Human Leukocyte and Lymphocyte Subsets. *Frontiers in Immunology*, *10*, 2434. https://doi.org/10.3389/fimmu.2019.02434

Karimian, A., Azizian, K., Parsian, H., Rafieian, S., Shafiei-Irannejad, V., Kheyrollah, M., Yousefi, M., Majidinia, M., & Yousefi, B. (2019). CRISPR/Cas9 technology as a potent molecular tool for gene therapy. *Journal of Cellular Physiology*, *234*(8), 12267–12277. https://doi.org/10.1002/jcp.27972

Kikkawa, M., & Yanagisawa, H. (2022). Identifying proteins in the cell by tagging techniques for cryo-electron microscopy. *Microscopy (Oxford, England)*, *71*(Supplement_1), i60–i65. https://doi.org/10.1093/jmicro/dfab059

Kim, J. M., Yi, E., Cho, H., Choi, W. S., Ko, D.-H., Yoon, D. H., Hwang, S.-H., & Kim, H. S. (2020). Assessment of NK Cell Activity Based on NK Cell-Specific Receptor Synergy in Peripheral Blood Mononuclear Cells and Whole Blood. *International Journal of Molecular Sciences*, *21*(21), Article 21. https://doi.org/10.3390/ijms21218112

Koh, C.-H., Lee, S., Kwak, M., Kim, B.-S., & Chung, Y. (2023). CD8 T-cell subsets: Heterogeneity, functions, and therapeutic potential. *Experimental & Molecular Medicine*, *55*(11), 2287–2299. https://doi.org/10.1038/s12276-023-01105-x

Koster, A. J., & Klumperman, J. (2003). Electron microscopy in cell biology: Integrating structure and function. *Nature Reviews. Molecular Cell Biology*, *Suppl*, SS6-10.

Krężel, A., & Maret, W. (2021). The Bioinorganic Chemistry of Mammalian Metallothioneins. *Chemical Reviews*, *121*(23), 14594–14648. https://doi.org/10.1021/acs.chemrev.1c00371

Lau, C.-H., Tin, C., & Suh, Y. (2020). CRISPR-based strategies for targeted transgene knock-in and gene correction. *Faculty Reviews*, *9*, 20. https://doi.org/10.12703/r/9-20

Lee, P. Y., Costumbrado, J., Hsu, C.-Y., & Kim, Y. H. (2012). Agarose Gel Electrophoresis for the Separation of DNA Fragments. *JoVE (Journal of Visualized Experiments)*, *62*, e3923. https://doi.org/10.3791/3923

Li, X., Jin, J., Guo, Z., & Liu, L. (2022). Evolution of plasmid-construction. *International Journal of Biological Macromolecules*, *209*, 1319–1326. https://doi.org/10.1016/j.ijbiomac.2022.04.094

Li, X., Liu, H., Wang, Y., Crabbe, M. J. C., Wang, L., Ma, W., & Ren, Z. (2024). Preparation of a novel metallothionein-AuNP composite material by genetic modification and AuS covalent combination. *International Journal of Biological Macromolecules*, *262*, 129960. https://doi.org/10.1016/j.ijbiomac.2024.129960

Liu, H., Wang, S., Xin, J., Wang, J., Yao, C., & Zhang, Z. (2019). Role of NKG2D and its ligands in cancer immunotherapy. *American Journal of Cancer Research*, *9*(10), 2064–2078.

Liu, S.-L., Wang, Z.-G., Xie, H.-Y., Liu, A.-A., Lamb, D. C., & Pang, D.-W. (2020). Single-Virus Tracking: From Imaging Methodologies to Virological Applications. *Chemical Reviews*, *120*(3), 1936–1979. https://doi.org/10.1021/acs.chemrev.9b00692

Lundberg, E., & Borner, G. H. H. (2019). Spatial proteomics: A powerful discovery tool for cell biology. *Nature Reviews Molecular Cell Biology*, *20*(5), 285–302. https://doi.org/10.1038/s41580-018-0094-y

Mali, P., Yang, L., Esvelt, K. M., Aach, J., Guell, M., DiCarlo, J. E., Norville, J. E., & Church, G. M. (2013). RNA-Guided Human Genome Engineering via Cas9. *Science*, *339*(6121), 823–826. https://doi.org/10.1126/science.1232033

Martell, J. D., Deerinck, T. J., Lam, S. S., Ellisman, M. H., & Ting, A. Y. (2017). Electron microscopy using the genetically encoded APEX2 tag in cultured mammalian cells. *Nature Protocols*, *12*(9), 1792–1816. https://doi.org/10.1038/nprot.2017.065

Martell, J. D., Deerinck, T. J., Sancak, Y., Poulos, T. L., Mootha, V. K., Sosinsky, G. E., Ellisman, M. H., & Ting, A. Y. (2012). Engineered ascorbate peroxidase as a genetically encoded reporter for electron microscopy. *Nature Biotechnology*, *30*(11), 1143–1148. https://doi.org/10.1038/nbt.2375

McIntosh, J. R. (2001). Electron Microscopy of Cells: A New Beginning for a New Century. *Journal of Cell Biology*, *153*(6), F25–F32. https://doi.org/10.1083/jcb.153.6.F25

McKinnon, K. M. (2018). Flow Cytometry: An Overview. *Current Protocols in Immunology*, *120*(1), 5.1.1-5.1.11. https://doi.org/10.1002/cpim.40

Montante, S., & Brinkman, R. R. (2019). Flow cytometry data analysis: Recent tools and algorithms. *International Journal of Laboratory Hematology*, *41*(S1), 56–62. https://doi.org/10.1111/ijlh.13016

Morphew, M. k., O'toole, E. t., Page, C. l., Pagratis, M., Meehl, J., Giddings, T., Gardner, J. m., Ackerson, C., Jaspersen, S. l., Winey, M., Hoenger, A., & Mcintosh, J. r. (2015). Metallothionein as a clonable tag for protein localization by electron microscopy of cells. *Journal of Microscopy*, *260*(1), 20–29. https://doi.org/10.1111/jmi.12262

Mu, W., Zhang, Y., Xue, X., Liu, L., Wei, X., & Wang, H. (2019). 5′ capped and 3′ polyA-tailed sgRNAs enhance the efficiency of CRISPR-Cas9 system. *Protein & Cell*, *10*(3), 223–228. https://doi.org/10.1007/s13238-018-0552-5

Newstead, S., & Barr, F. (2020). Molecular basis for KDEL-mediated retrieval of escaped ER-resident proteins – SWEET talking the COPs. *Journal of Cell Science*, *133*(19), jcs250100. https://doi.org/10.1242/jcs.250100

Patel, B. (2009). Simple, Fast, and Efficient Cloning of PCR Products with TOPO® Cloning Vectors. *BioTechniques*, *46*(7), 559. https://doi.org/10.2144/000113200

Ramzan, R., Kadenbach, B., & Vogt, S. (2021). Multiple Mechanisms Regulate Eukaryotic Cytochrome C Oxidase. *Cells*, *10*(3), Article 3. https://doi.org/10.3390/cells10030514

Ran, F. A., Hsu, P. D., Lin, C.-Y., Gootenberg, J. S., Konermann, S., Trevino, A. E., Scott, D. A., Inoue, A., Matoba, S., Zhang, Y., & Zhang, F. (2013). Double Nicking by RNA-Guided CRISPR Cas9 for Enhanced Genome Editing Specificity. *Cell*, *154*(6), 1380–1389. https://doi.org/10.1016/j.cell.2013.08.021

Ran, F. A., Hsu, P. D., Wright, J., Agarwala, V., Scott, D. A., & Zhang, F. (2013). Genome engineering using the CRISPR-Cas9 system. *Nature Protocols*, *8*(11), 2281–2308. https://doi.org/10.1038/nprot.2013.143

Reina-Campos, M., Scharping, N. E., & Goldrath, A. W. (2021). CD8+ T cell metabolism in infection and cancer. *Nature Reviews Immunology*, *21*(11), 718–738. https://doi.org/10.1038/s41577-021-00537-8

Rotko, D., Kudin, A. P., Zsurka, G., Kulawiak, B., Szewczyk, A., & Kunz, W. S. (2021). Molecular and Functional Effects of Loss of Cytochrome c Oxidase Subunit 8A. *Biochemistry (Moscow)*, *86*(1), 33–43. https://doi.org/10.1134/S0006297921010041

S. Makarova, K., H. Haft, D., Barrangou, R., J. J. Brouns, S., Charpentier, E., Horvath, P., Moineau, S., J. M. Mojica, F., I. Wolf, Y., Yakunin, A. F., van der Oost, J., & V. Koonin, E. (2011).

Evolution and classification of the CRISPR-Cas systems. *Nature Reviews. Microbiology*, *9*(6), 467–477. https://doi.org/10.1038/nrmicro2577

Sachse, M., de Castro, I. F., Tenorio, R., & Risco, C. (2024). Molecular mapping of virus-infected cells with immunogold and metal-tagging transmission electron microscopy. *Molecular Microbiology*, *121*(4), 688–695. https://doi.org/10.1111/mmi.15182

Samuel, M. S., Datta, S., Khandge, R. S., & Selvarajan, E. (2021). A state of the art review on characterization of heavy metal binding metallothioneins proteins and their widespread applications. *Science of The Total Environment*, *775*, 145829. https://doi.org/10.1016/j.scitotenv.2021.145829

Sengupta, R., Poderycki, M. J., & Mattoo, S. (2019). CryoAPEX – an electron tomography tool for subcellular localization of membrane proteins. *Journal of Cell Science*, *132*(6), jcs222315. https://doi.org/10.1242/jcs.222315

Sherba, J. J., Hogquist, S., Lin, H., Shan, J. W., Shreiber, D. I., & Zahn, J. D. (2020). The effects of electroporation buffer composition on cell viability and electro-transfection efficiency. *Scientific Reports*, *10*(1), 3053. https://doi.org/10.1038/s41598-020-59790-x

Shigemoto, R. (2022). Electron microscopic visualization of single molecules by tag-mediated metal particle labeling. *Microscopy*, *71*(Supplement_1), i72–i80. https://doi.org/10.1093/jmicro/dfab048

Smirnikhina, S. A., Anuchina, A. A., & Lavrov, A. V. (2019). Ways of improving precise knock-in by genome-editing technologies. *Human Genetics*, *138*(1), 1–19. https://doi.org/10.1007/s00439-018-1953-5

Stephan, T., Roesch, A., Riedel, D., & Jakobs, S. (2019). Live-cell STED nanoscopy of mitochondrial cristae. *Scientific Reports*, *9*(1), 12419. https://doi.org/10.1038/s41598-019-48838-2

Strong, A., & Musunuru, K. (2017). Genome editing in cardiovascular diseases. *Nature Reviews Cardiology*, *14*(1), 11–20. https://doi.org/10.1038/nrcardio.2016.139

Syaifudin, M. (2021). Gel electrophoresis: The applications and its improvement with nuclear technology. *AIP Conference Proceedings*, *2331*(1), 050008. https://doi.org/10.1063/5.0042067

Tapia, D., Jiménez, T., Zamora, C., Espinoza, J., Rizzo, R., González-Cárdenas, A., Fuentes, D., Hernández, S., Cavieres, V. A., Soza, A., Guzmán, F., Arriagada, G., Yuseff, M. I., Mardones, G. A., Burgos, P. V., Luini, A., González, A., & Cancino, J. (2019). KDEL receptor regulates secretion by lysosome relocation- and autophagy-dependent modulation of lipid-droplet turnover. *Nature Communications*, *10*(1), 735. https://doi.org/10.1038/s41467-019-08501-w

Thirumoorthy, N., Manisenthil Kumar, K., Shyam Sundar, A., Panayappan, L., & Chatterjee, M. (2007). Metallothionein: An overview. *World Journal of Gastroenterology : WJG*, *13*(7), 993–996. https://doi.org/10.3748/wjg.v13.i7.993

Thomas, S., Maynard, N. D., & Gill, J. (2015). DNA library construction using Gibson Assembly®. *Nature Methods*, *12*(11), i–ii. https://doi.org/10.1038/nmeth.f.384

Vázquez-Gutiérrez, J. L., & Langton, M. (2015). Current potential and limitations of immunolabeling in cereal grain research. *Trends in Food Science & Technology*, *41*(2), 105–117. https://doi.org/10.1016/j.tifs.2014.10.002

Voytas, D. (2000). Agarose Gel Electrophoresis. *Current Protocols in Molecular Biology*, *51*(1), 2.5A.1-2.5A.9. https://doi.org/10.1002/0471142727.mb0205as51

Wang, D., Tai, P. W. L., & Gao, G. (2019). Adeno-associated virus vector as a platform for gene therapy delivery. *Nature Reviews. Drug Discovery*, *18*(5), 358–378. https://doi.org/10.1038/s41573-019-0012-9

Wardyn, J. D., Chan, A. S. Y., & Jeyasekharan, A. D. (2021). A Robust Protocol for CRISPR-Cas9 Gene Editing in Human Suspension Cell Lines. *Current Protocols*, *1*(11), e286. https://doi.org/10.1002/cpz1.286

Watanabe, G., & Lieber, M. R. (2023). The flexible and iterative steps within the NHEJ pathway. *Progress in Biophysics and Molecular Biology*, *180–181*, 105–119. https://doi.org/10.1016/j.pbiomolbio.2023.05.001

Wires, E. S., Trychta, K. A., Kennedy, L. M., & Harvey, B. K. (2021). The Function of KDEL Receptors as UPR Genes in Disease. *International Journal of Molecular Sciences*, *22*(11), Article 11. https://doi.org/10.3390/ijms22115436

Xiong, X., Chen, M., Lim, W. A., Zhao, D., & Qi, L. S. (2016). CRISPR/Cas9 for Human Genome Engineering and Disease Research. *Annual Review of Genomics and Human Genetics*, *17*(Volume 17, 2016), 131–154. https://doi.org/10.1146/annurev-genom-083115-022258

Xu, F., Jiang, M., Li, D., Yu, P., Ma, H., & Lu, H. (2024). Protective effects of antibiotic resistant bacteria on susceptibles in biofilm: Influential factors, mechanism, and modeling. *Science of The Total Environment*, *930*, 172668. https://doi.org/10.1016/j.scitotenv.2024.172668

Xu, Y., & Li, Z. (2020). CRISPR-Cas systems: Overview, innovations and applications in human disease research and gene therapy. *Computational and Structural Biotechnology Journal*, *18*, 2401–2415. https://doi.org/10.1016/j.csbj.2020.08.031